

Synchrotron Radiation and Vacuum Issues for the FCC-ee Machine Detector Interface Region

R. Kersevan, VSC Seminar, 31/10/2023

OUTLINE

- FCC study program (2013-today)
- FCC-ee: relevant machine and vacuum parameters
- Vacuum chamber cross section
- Synchrotron radiation spectrum, flux, power
- SR absorbers: yes or no?
- Pumping solutions
- **The MDI region**
- Synchrotron radiation ray-tracing
- Pressure profiles
- Future work and conclusions
- Acknowledgments

Relevant machine and vacuum parameters (pre-2019)

Eur. Phys. J. Special Topics 228, 261–623 (2019)
 © The Author(s) 2019
<https://doi.org/10.1140/epjst/e2019-900045-4>

THE EUROPEAN
 PHYSICAL JOURNAL
 SPECIAL TOPICS

Regular Article

FCC-ee: The Lepton Collider

Future Circular Collider Conceptual Design Report Volume 2

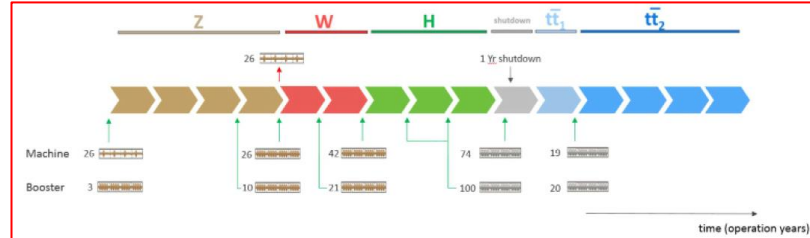


Fig. 4. FCC-ee operation time line. The bottom part indicates the number of cryomodules to be installed in the collider and booster, respectively, during the various winter shutdown periods; also see [22].

Table 1. Machine parameters of the FCC-ee for different beam energies.

	Z	WW	ZH	tt	
Circumference (km)			97.756		
Bending radius (km)			10.760		
Free length to IP l^* (m)			2.2		
Solenoid field at IP (T)			2.0		
Full crossing angle at IP θ (mrad)			30		
SR power/beam (MW)			50		
Beam energy (GeV)	45.6	80	120	175	182.5
Beam current (mA)	1390	147	29	6.4	5.4
Bunches/beam	16 640	2000	328	59	48

292

The European Physical Journal Special Topics

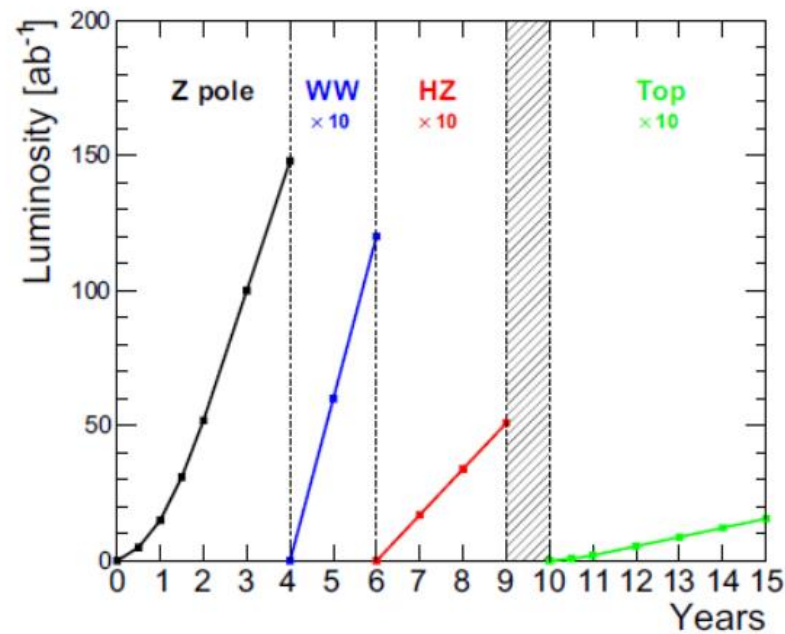


Fig. 1.2. Operation model for the FCC-ee, as a result of the five-year conceptual design study, showing the integrated luminosity at the Z pole (black), the WW threshold (blue), the Higgs factory (red), and the top-pair threshold (green) as a function of time. The hatched area indicates the shutdown time needed to prepare the collider for the highest energy runs.

Big variation of nominal current vs beam energy, since all machine versions are **limited to 50 MW of synchrotron radiation per beam**

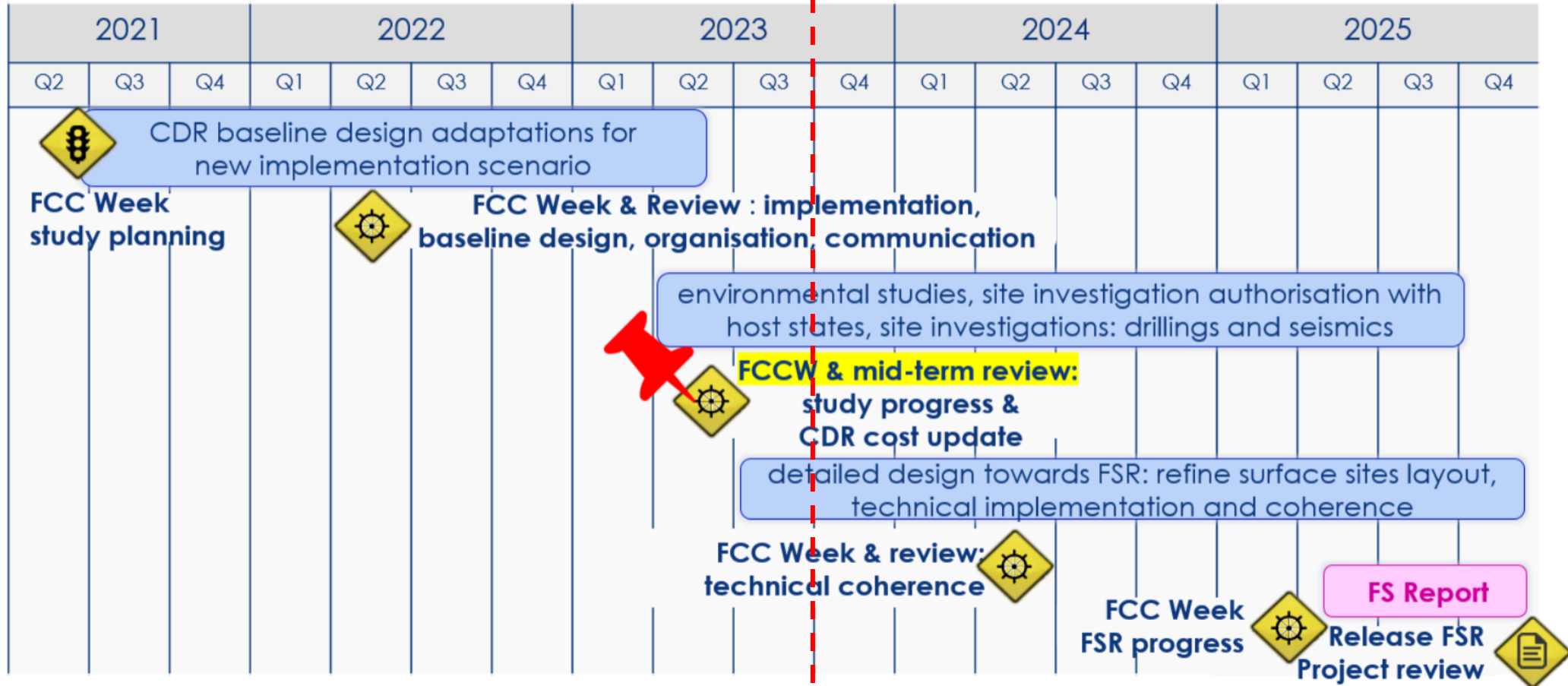
$$P(W) = 88.46 \cdot E^4(\text{GeV}) \cdot I(\text{mA}) / \rho(\text{m}) \leftarrow 50 \text{ MW/beam MAX}$$

$$F(\text{ph/s}) = 8.08 \cdot 10^{17} \cdot E(\text{GeV}) \cdot I(\text{mA})$$

- We aim at an average pressure giving a beam-gas scattering lifetime large enough not to be detrimental to the integrated luminosity, say in the low 10-9 mbar range, or better, with a gas composition of 80~90% hydrogen, and no molecular masses above 44 (CO_2).
- We also aim at reducing/eliminating the e-cloud and ion-trapping effects and related beam instabilities and losses
- Typically, we assume a residual gas composition of 80~90% H_2 , 10~20% $\text{CO}+\text{CO}_2$, traces of CH_4



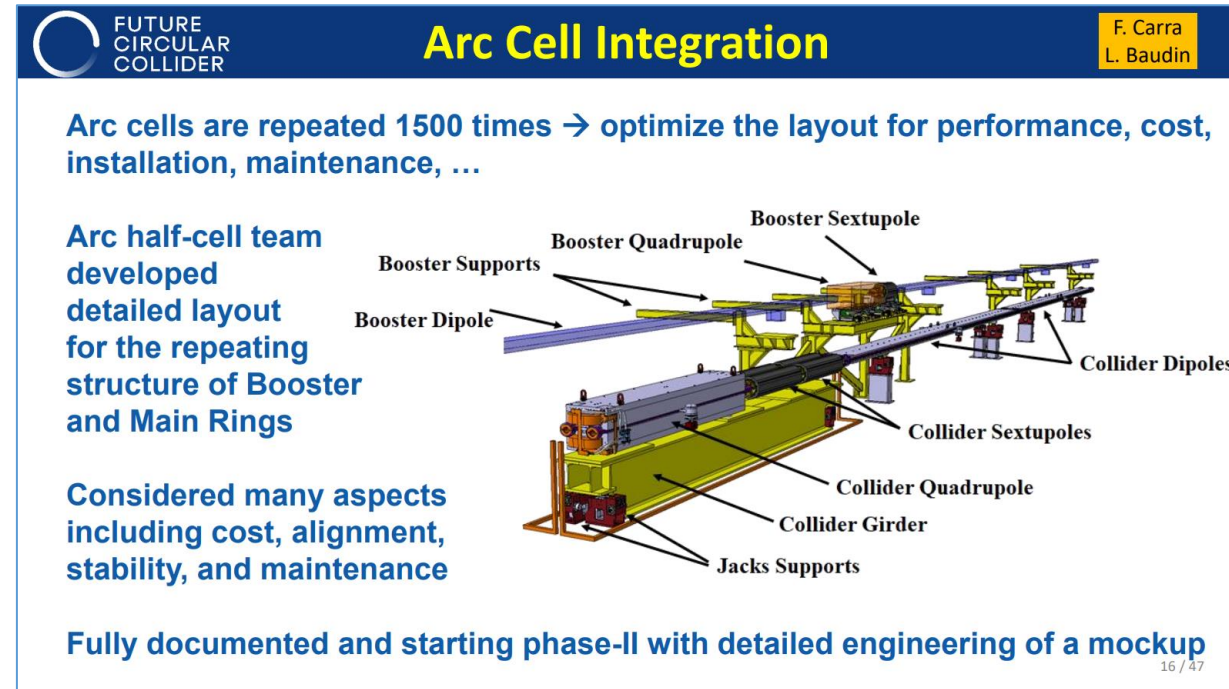
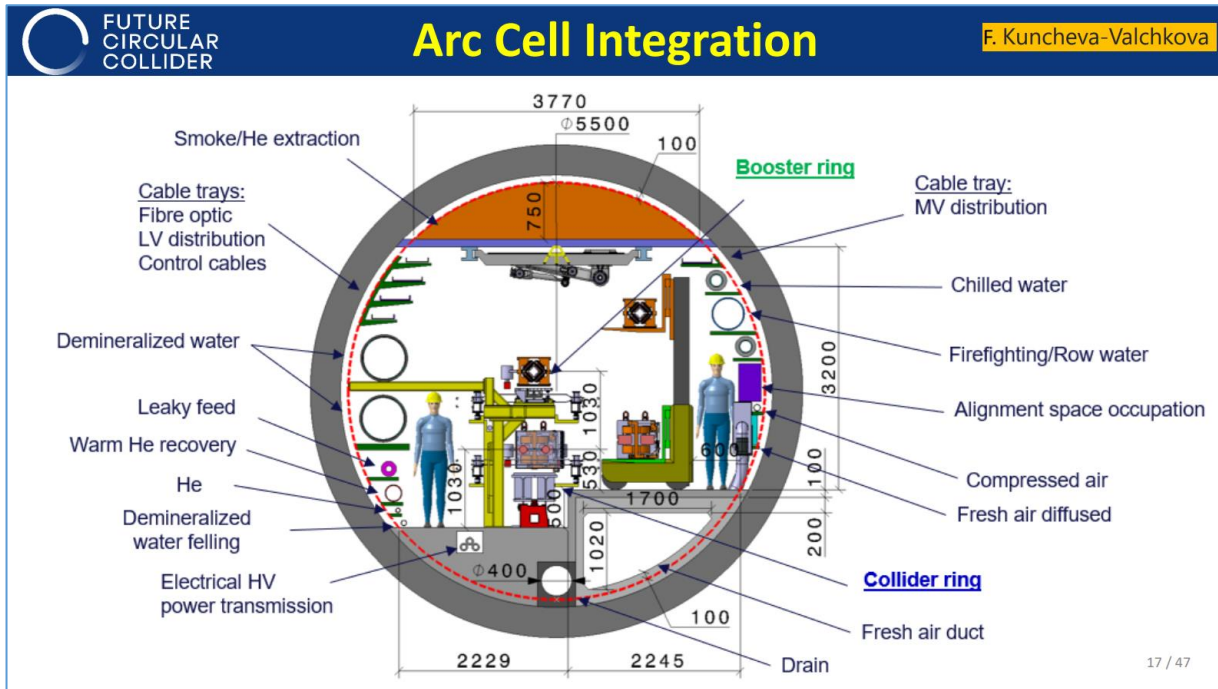
Feasibility Study Timeline and main activities/milestones



- FCC-ee is a very large machine ↓
- It is highly modular, i.e. most of the length of the machine is a repetition of a “basic cell”
- There is a large margin of cost-optimization and industrialization of most components: vacuum chambers, bellows, beam-position monitor blocks, flanges, RF-contact fingers, etc...
- The prototyping phase has already started, exploring new technologies (e.g. additive manufacturing, see examples below)

Parameter	unit	2018 CDR [1]	2023 Optimised
Total circumference	km	97.75	90.657
Total arc length	km	83.75	76.93
Arc bending radius	km	13.33	12.24
Arc lengths (and number)	km	8.869 (8), 3.2 (4)	9.617 (8)
Number of surface sites	—	12	8
Number of straights	—	8	8
Length (and number) of straights	km	1.4 (6), 2.8 (2)	1.4 (4), 2.031 (4)
superperiodicity	—	2	4

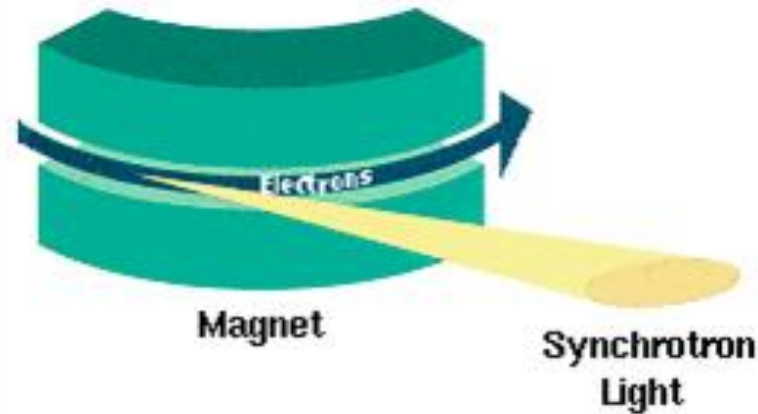
- The tunnel along the arcs has a typical cross-section as shown below (left)



- There are TWO counter-rotating beams (e- and e+) guided by dipole, quadrupole, and sextupole magnets (above, right)
- Above the two rings of the collider, there is a THIRD ring, the full-energy injection BOOSTER, which injects both e- and e+ (in opposite directions) whenever necessary
- There are, therefore, about 3x 91 km ring vacuum system, plus additional (many) km of TRANSFER LINES (TLs) from booster to collider rings, and also other TLs from other accelerators in the chain (pre-booster chain has different options under study)

- The vacuum chamber geometry is strongly linked to the design of the magnets
- We need to pump out all air molecules present inside the vacuum chamber after installation, and then also all of the molecules which are generated via several physical effects, such as PHOTODESORPTION, ELECTRON CLOUD, RESISTIVE WALL HEATING, BEAM LOSSES, and more...
- We need to remove as many RESIDUAL GAS molecules as possible, to avoid their collision with the stored e- and e+ beams
- The typical average pressure compatible with the correct functioning of the collider is “few” 10^{-9} mbar (10^{-10} mbar in the INTERACTION REGION, where collisions occur)
- In order to get below this pressure value, we adopt state-of-the-art technologies, several of them invented at CERN in the past, and new ones under development now
- **Challenge**: applying these technologies to “regular” accelerators (i.e. having circumferences of ~500-1000 m) is rather easy albeit costly; now we need to reduce costs without compromising on quality. **Plenty of opportunities for industrial optimisation.**

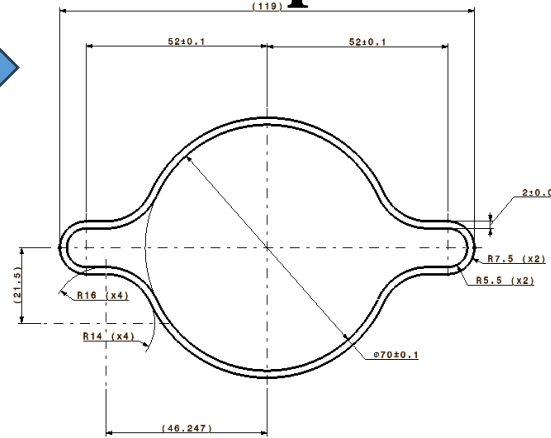
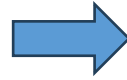
- One of the main sources of RESIDUAL GAS is the **synchrotron radiation (SR)-induced outgassing**
- SR is the emission of **intense electromagnetic radiation when an energetic charged particle moves in a strong magnetic field**: it is a “searchlight” beam of photons with energy between microwaves and gamma rays (very energetic and penetrating)



- Upon striking the vacuum chamber wall, SR “pulls out” some molecules, which must be removed as fast as possible, to avoid interference with the beam
- The FCC-ee machines are all designed to generate a maximum of **50 MW of SR power per beam** (i.e. 100 MW of unavoidable “waste heat”)
- **All vacuum components hit by SR need therefore to be carefully designed and cooled**

Prototyping of vacuum components

- The vacuum chamber cross section in the arcs is



- It is made out of **extruded copper alloy**; it will be NEG-coated and every 5.5~6 m there will be a **SR PHOTON ABSORBER (SRA)** which will intercept the SR generated along the preceding dipole magnets.
- The design of the SRAs is **very demanding**, because each of them will receive a highly collimated SR fan, with **very high surface power density**
- In addition, the SRAs must satisfy some **geometrical criteria** which make their design challenging: we are prototyping some innovative design implementing **ADDITIVE MANUFACTURING** (3D printing) and **STIR-WELDING** technology, with **SHAPE-MEMORY ALLOY** rings for joining the different vacuum chamber segments and bulk **COLD-SPRAY DEPOSITION** for selected components
- Upon selection of the most suitable technology, we will look for INDUSTRIAL PARTNERS capable to deliver large quantities of these components in a TIMELY FASHION, following STRICT QUALITY CONTROL procedures**

Plasma-sprayed “bosses” for machining the BPM button electrodes

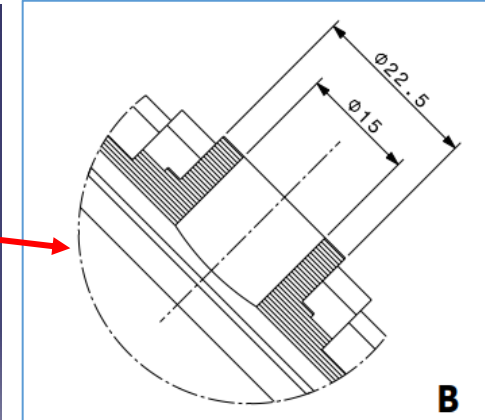
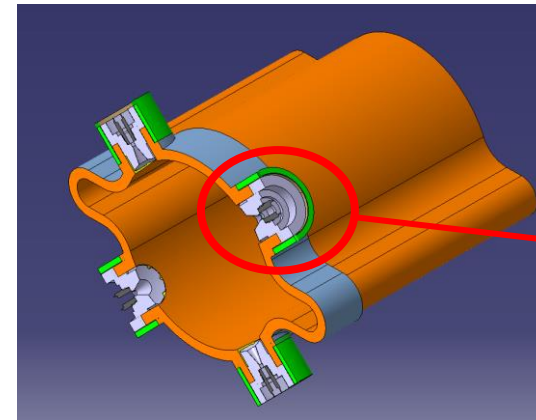
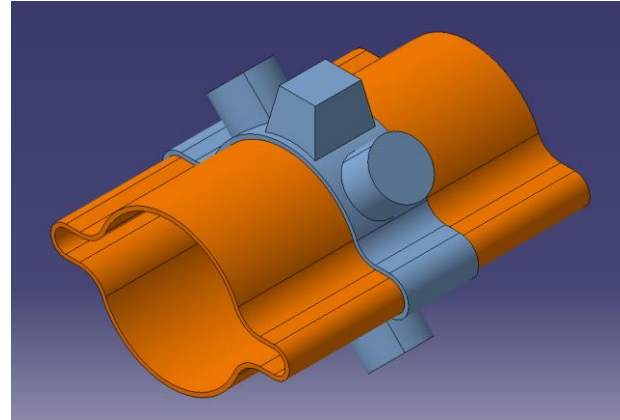
Friction stir welding of elliptical flanges to vacuum chamber extrusion



Chamber: 2mm layer sprayed all around

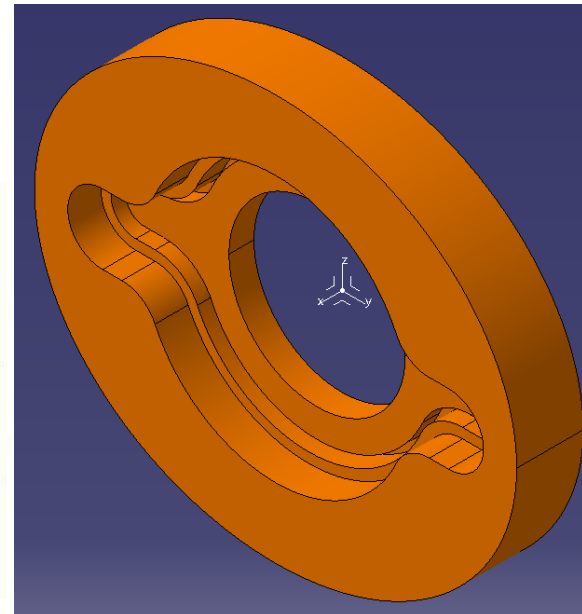
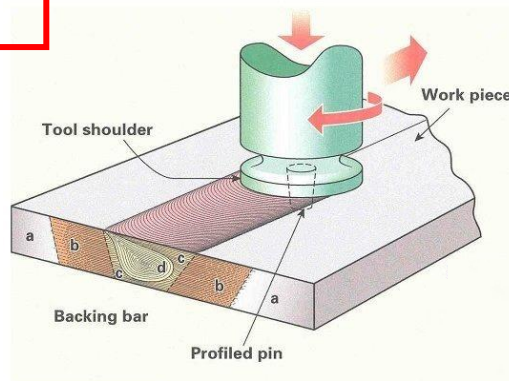


Chamber prototype with x4 bosses for direct BPM buttons machining and SMA rings

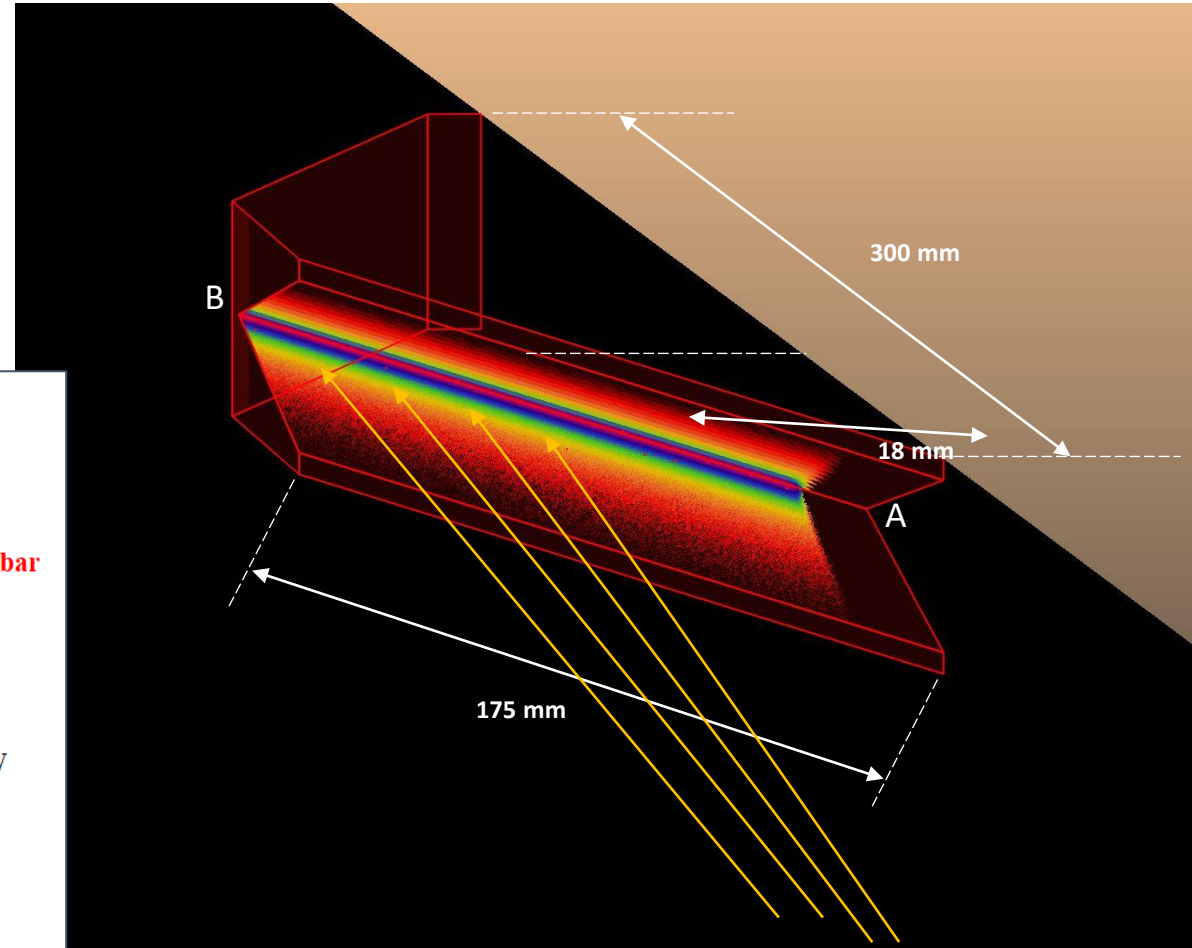
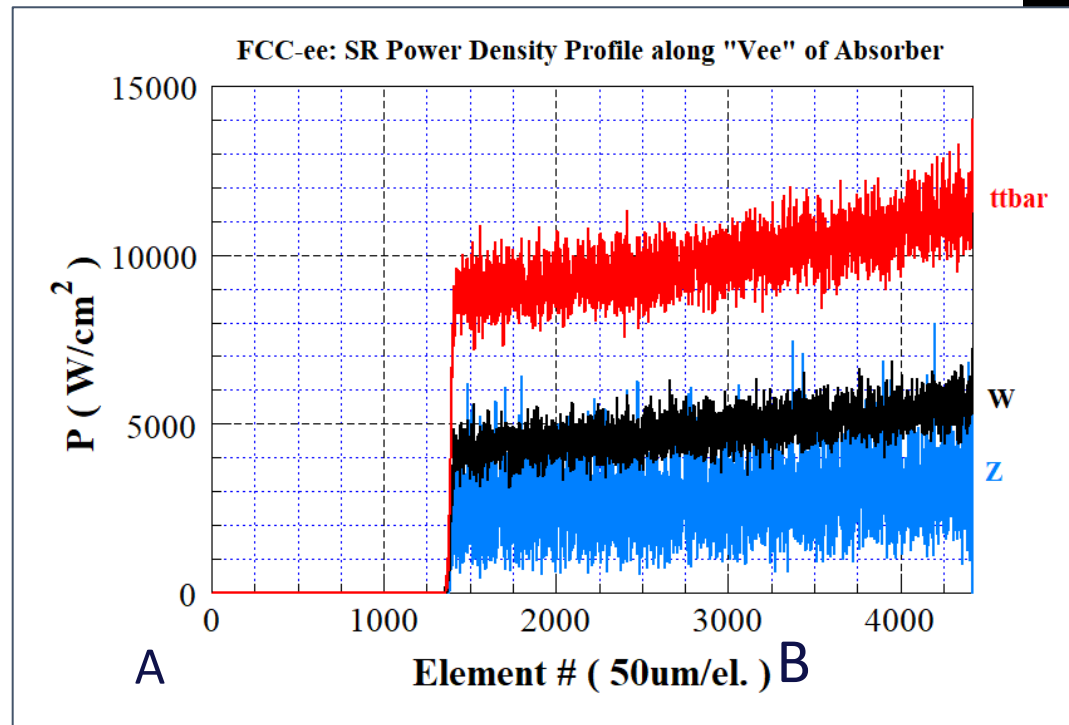
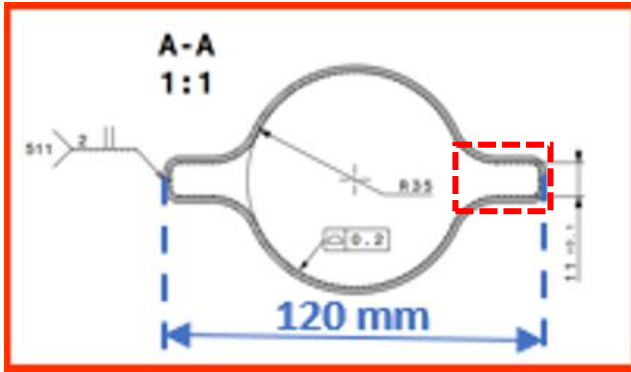


FRICITION STIR WELDING →

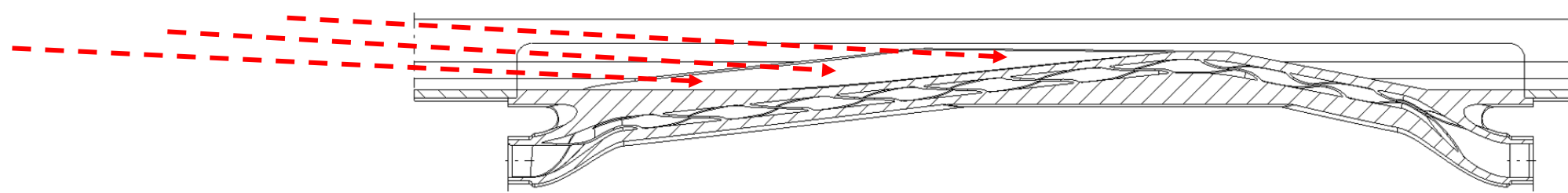
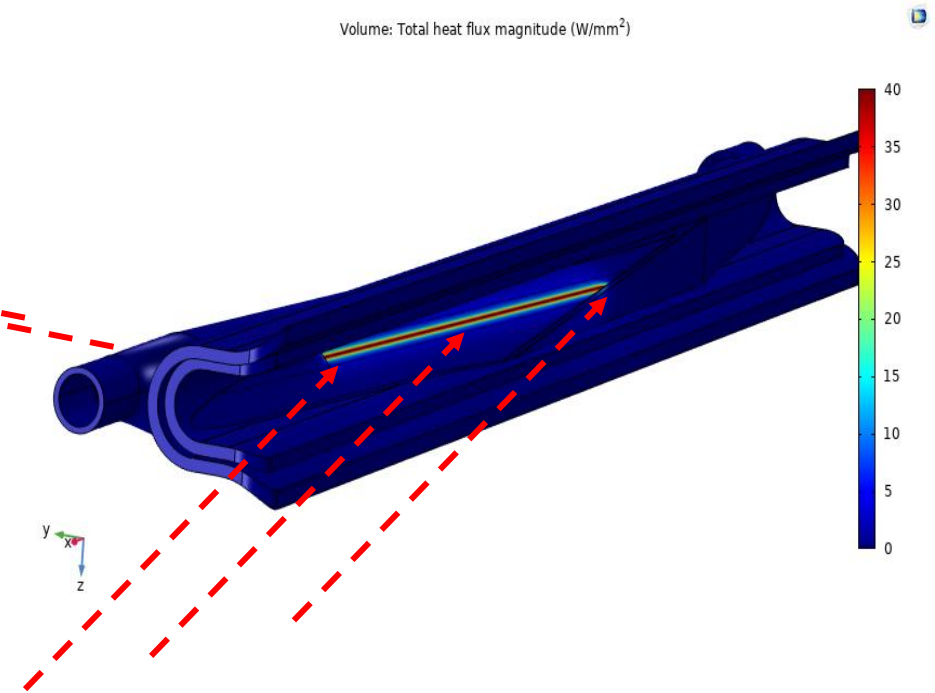
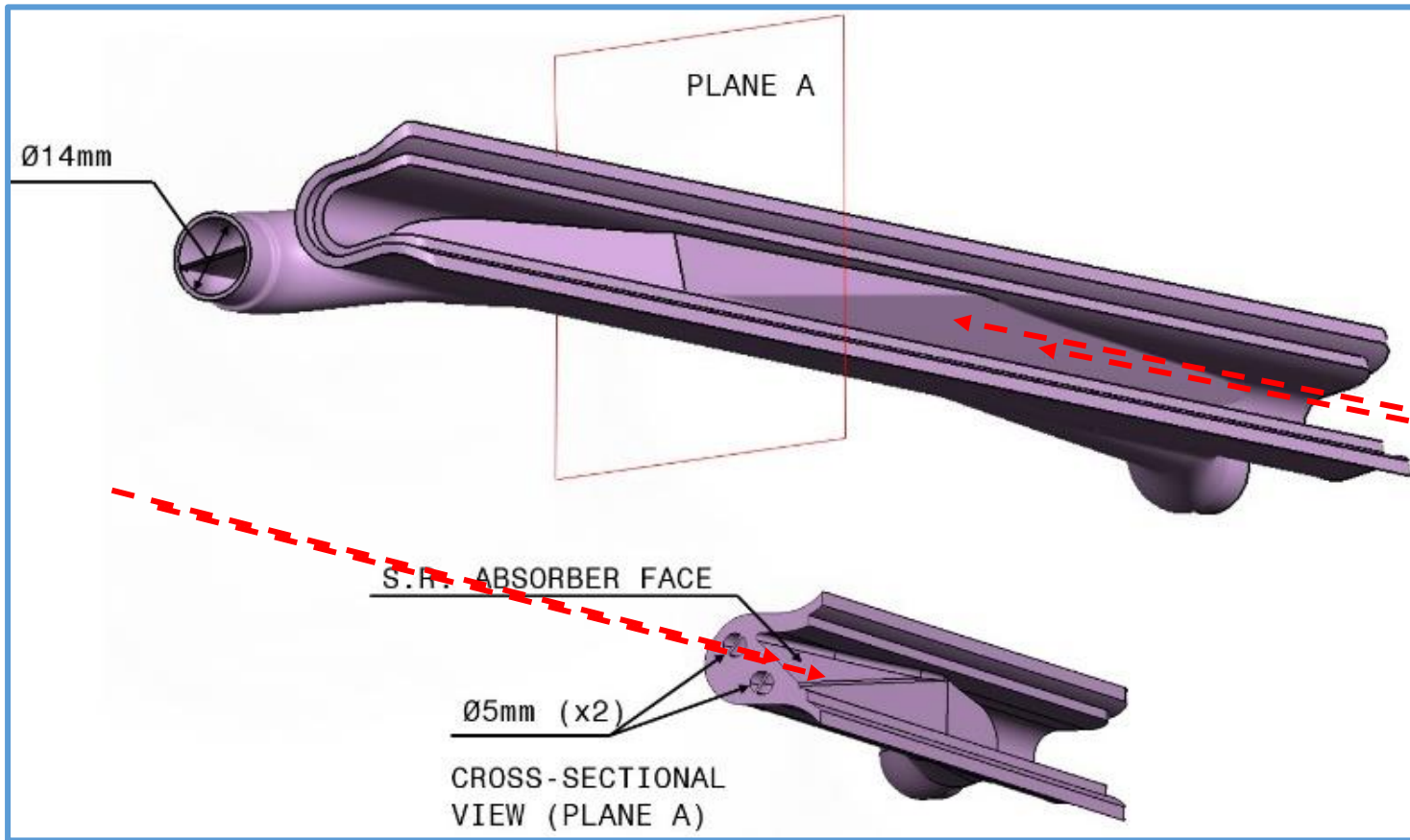
- Flange is redesigned as per Phase 1 results



Initial geometry of the SR photon absorber, now superseded by 3D-printed one (next slide)



Another example: 3D-PRINTED SR ABSORBER, with INTEGRATED COOLING CIRCUIT AND SWIRL TAPE TO IMPROVE HEAT EXCHANGE

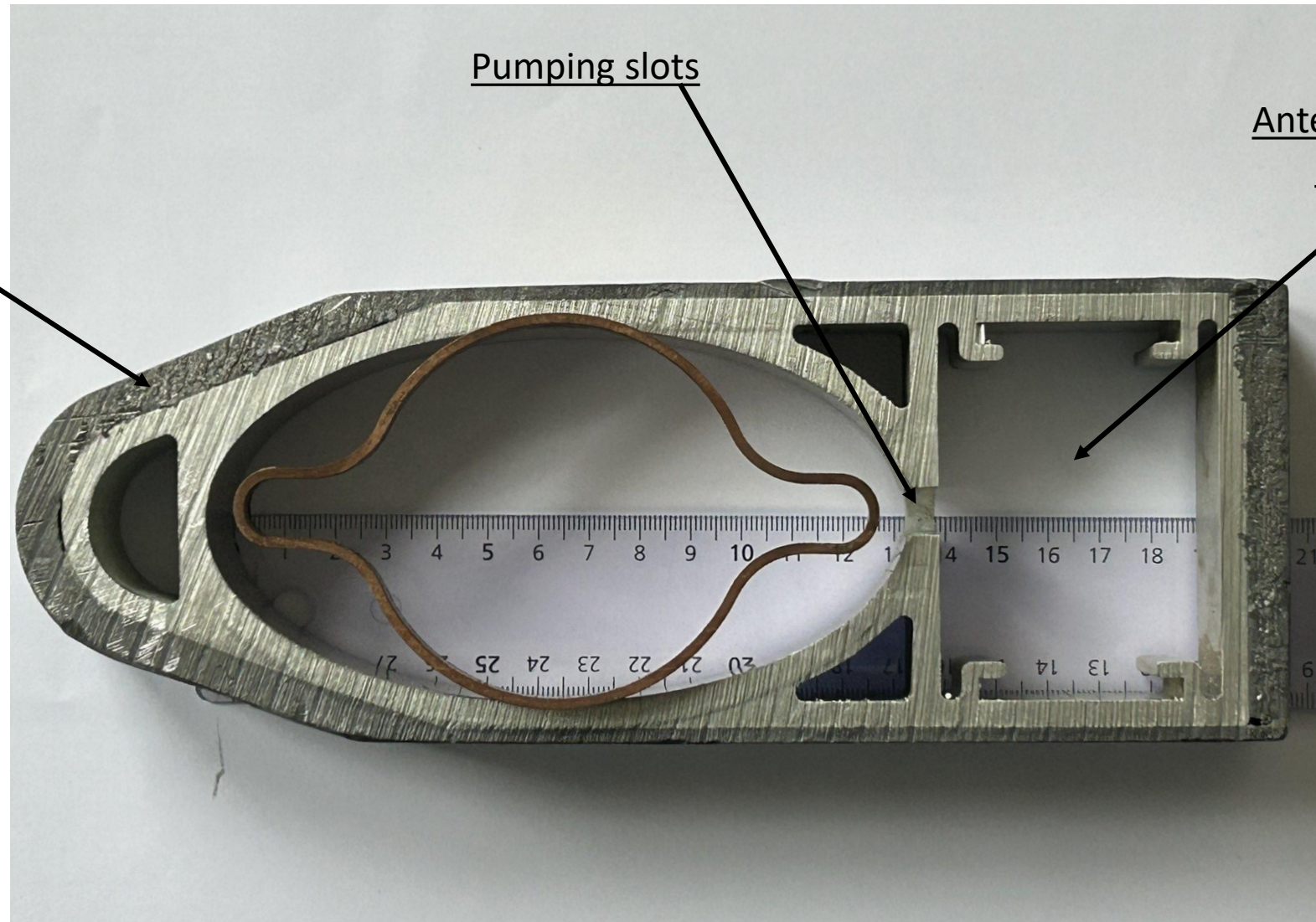


Comparison of LEP extruded cross-section (dipole chambers) with FCC-ee's

Lead shielding

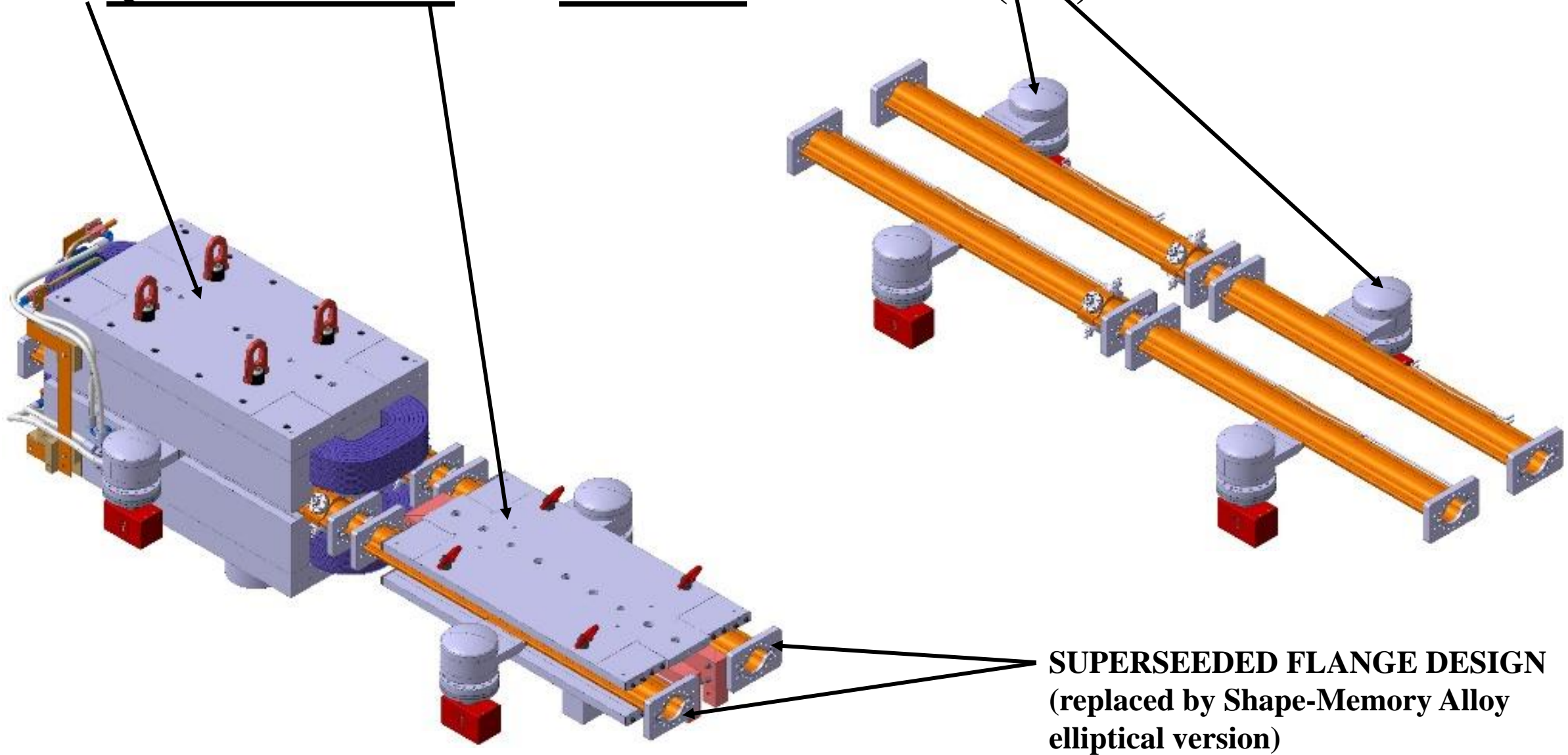
LEP:
ellipse 131x70 mm²

FCC-ee:
115 mm wide, 70 mm ID



The specific conductance of FCC-ee is $\sim 1/2$ that of LEP, $\sim 100:50$ l·m/s
The proposed 60 mm ID version for FCC-ee would have a 37% conductance decrease

View of the VACUUM CHAMBERS with PUMPING DOMES (right) and inside QUADRUPOLE and DIPOLE MAGNET (left)



FCC-hh beam screen and FCC-ee vacuum chamber prototype testing

BESTEX at KARA light source (Peter Lindquist Henriksen, formerly L.A. Gonzalez)

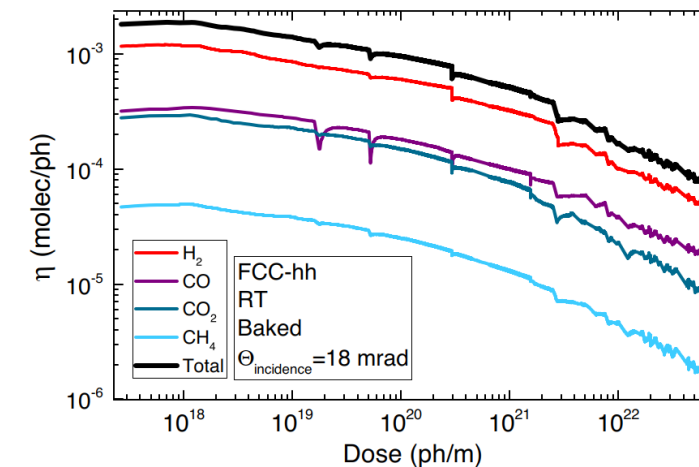
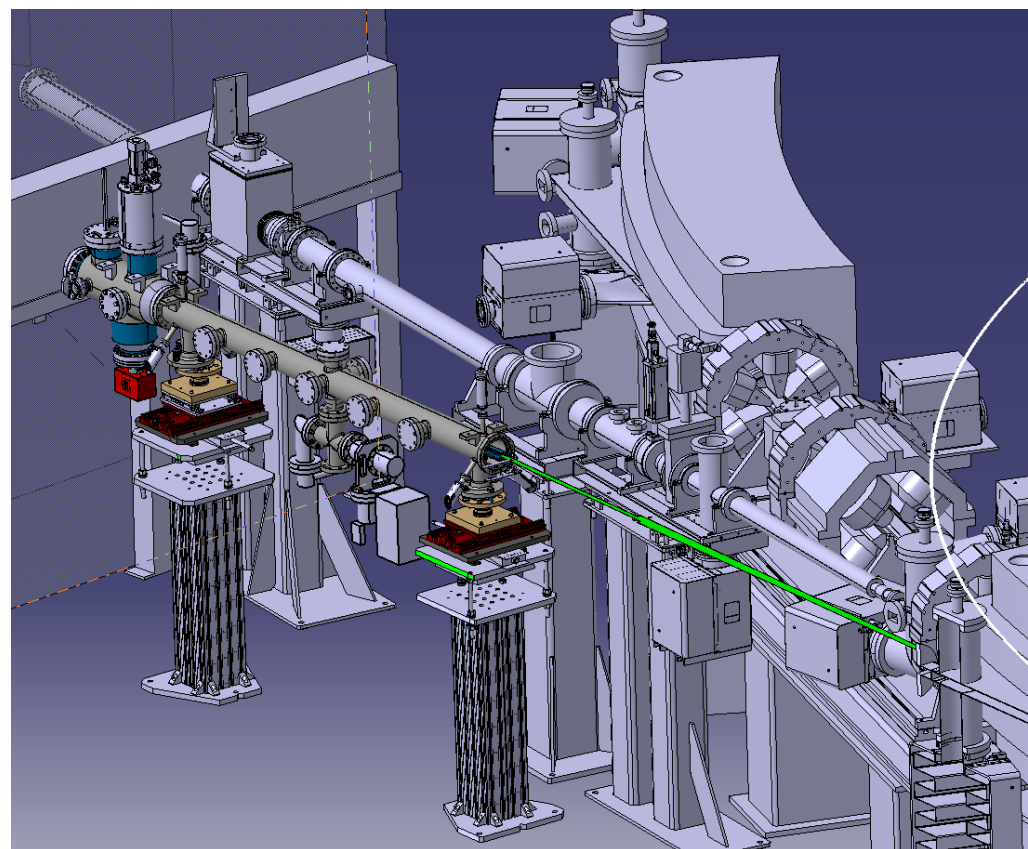
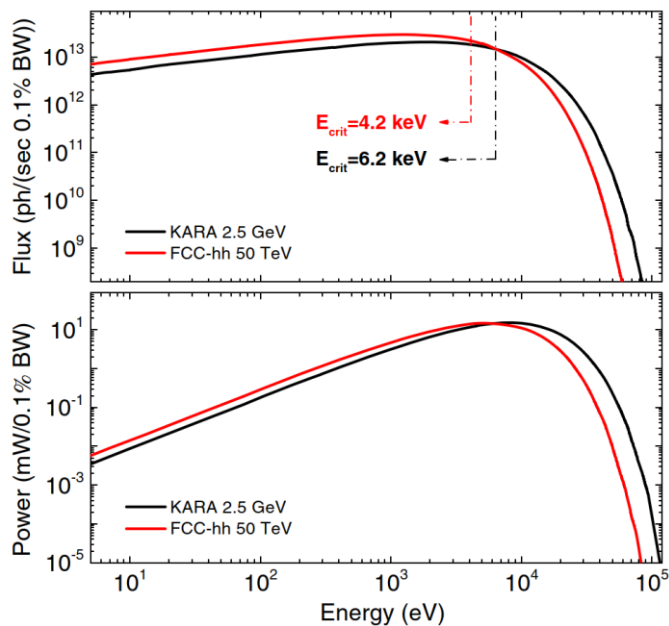


TABLE I. Comparison of the BESTEX (for the configuration of this specific work) and the FCC-hh relevant baseline parameters.

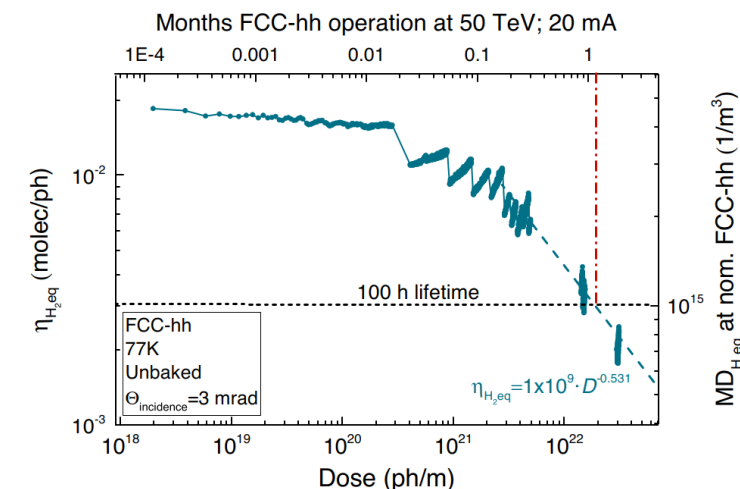
	BESTEX	FCC-hh
Critical energy [keV]	6.2	4.3
SR flux [ph/s/m]	4.84×10^{16}	1.7×10^{17}
SR power [W/m] ^a	32	32 ^b
Glancing angle [mrad]	18	1.35

^aPower received at the BS.

^bAverage value. Power ranges between 21 and 42 W/m.

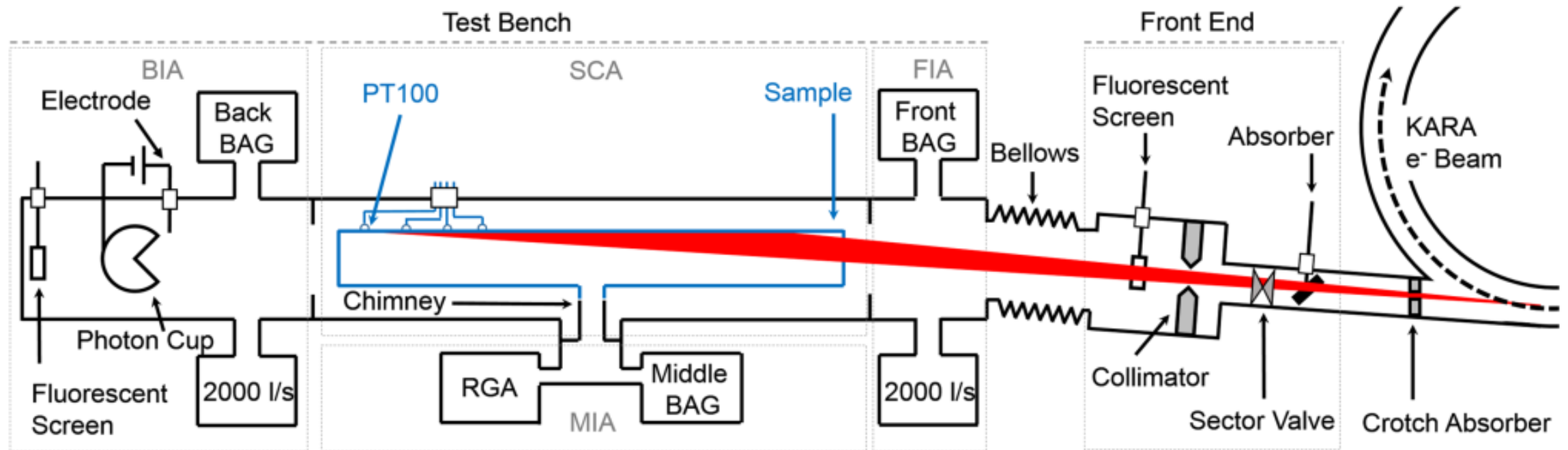
L. A. Gonzalez, et al. Commissioning of a beam screen test bench experiment with a future circular hadron collider type synchrotron radiation beam. DOI: 10.1103/PhysRevAccelBeams.22.083201

L. A. Gonzalez, et al. Photostimulated desorption performance of the future circular hadron collider beam screen. DOI: 10.1103/PhysRevAccelBeams.24.113201



This project has received funding from the European Union's Horizon Europe Research and Innovation programme under Grant Agreement No 101057511.

Schematics of BESTEX at KARA/KIT



- Machine parameters from official web page <http://tlep.web.cern.ch/content/machine-parameters>
- Very small vertical emittance for all energies
- High current (B-factory level) for Z-pole
- Luminosity lifetime t_{lum} dominates beam current decay, but vacuum lifetime must be at least several times longer than t_{lum} : good vacuum is a must

Consequence of 50 MW/beam MAX

$$P(W) = 88.46 \cdot E^4(\text{GeV}) \cdot I(\text{mA}) / \rho(\text{m})$$

$$F(\text{ph/s}) = 8.08 \cdot 10^{17} \cdot E(\text{GeV}) \cdot I(\text{mA})$$

The beam currents at the various energies scale as the reciprocal of the 4th power of the beam energy:

The beam current at ttbar is only $(45.6/182.5)^4 = 1/4^4 = 1/256$ that of the Z-pole

Old parameter table (97 km rings)

parameter	Z	W	H (ZH)	ttbar
beam energy [GeV]	45.6	80	120	182.5
arc cell optics	60/60	90/90	90/90	90/90
momentum compaction [10^{-5}]	1.48	0.73	0.73	0.73
horizontal emittance [nm]	0.27	0.28	0.63	1.45
vertical emittance [pm]	1.0	1.0	1.3	2.7
horizontal beta* [m]	0.15	0.2	0.3	1
vertical beta* [mm]	0.8	1	1	2
length of interaction area [mm]	0.42	0.5	0.9	1.99
tunes, half-ring (x, y, s)	(0.569, 0.61, 0.0125)	(0.577, 0.61, 0.0115)	(0.565, 0.60, 0.0180)	(0.553, 0.59, 0.0350)
longitudinal damping time [ms]	414	77	23	6.6
SR energy loss / turn [GeV]	0.036	0.34	1.72	9.21
total RF voltage [GV]	0.10	0.44	2.0	10.93
RF acceptance [%]	1.9	1.9	2.3	4.9
energy acceptance [%]	1.3	1.3	1.5	2.5
energy spread (SR / BS) [%]	0.038 / 0.132	0.066 / 0.153	0.099 / 0.151	0.15 / 0.20
bunch length (SR / BS) [mm]	3.5 / 12.1	3.3 / 7.65	3.15 / 4.9	2.5 / 3.3
Piwinski angle (SR / BS)	8.2 / 28.5	6.6 / 15.3	3.4 / 5.3	1.39 / 1.60
bunch intensity [10^{11}]	1.7	1.5	1.5	2.8
no. of bunches / beam	16640	2000	393	39
beam current [mA]	1390	147	29	5.4
luminosity [$10^{34} \text{ cm}^{-2} \text{ s}^{-1}$]	230	32	8	1.5
beam-beam parameter (x / y)	0.004 / 0.133	0.0065 / 0.118	0.016 / 0.108	0.094 / 0.150
luminosity lifetime [min]	70	50	42	44
time between injections [sec]	122	44	31	32
allowable asymmetry [%]	± 5	± 3	± 3	± 3
required lifetime by BS [min]	29	16	11	10
actual lifetime by BS ("weak") [min]	> 200	20	20	25

New parameter table (90.7 km rings)

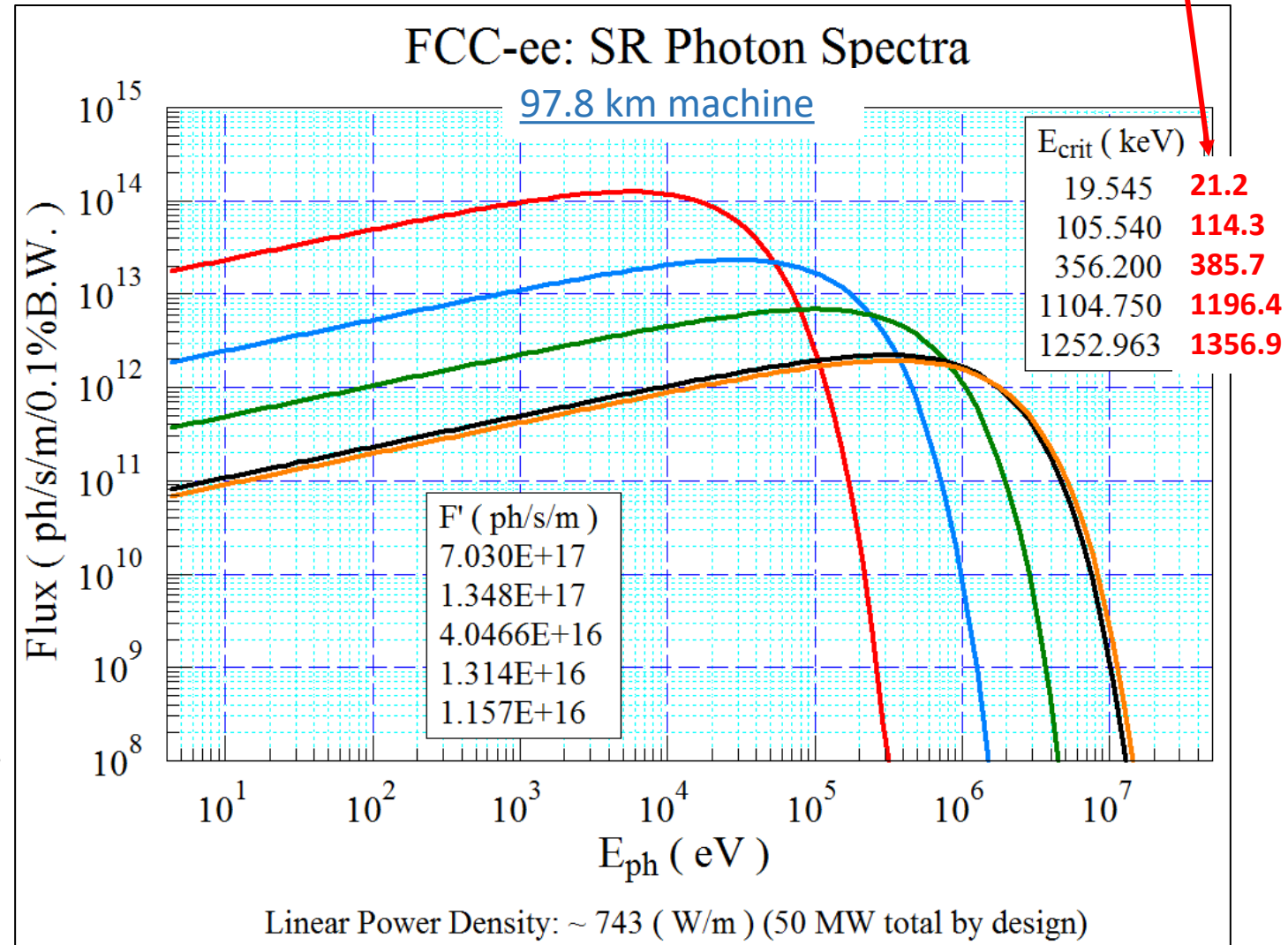
Parameters					
FCC-ee collider parameters as of June 3, 2023.					
Beam energy	[GeV]	45.6	80	120	182.5
Layout		PA31-3.0			
# of IPs		4			
Circumference	[km]	90.658816			
Bend. radius of arc dipole	[km]	9.936			
Energy loss / turn	[GeV]	0.0394	0.374	1.89	10.42
SR power / beam	[MW]	50			
Beam current	[mA]	1270	137	26.7	4.9
Colliding bunches / beam		15880	1780	440	60
Colliding bunch population	[10 ¹¹]	1.51	1.45	1.15	1.55
Hor. emittance at collision ε_x	[nm]	0.71	2.17	0.71	1.59
Ver. emittance at collision ε_y	[pm]	1.4	2.2	1.4	1.6
Lattice ver. emittance $\varepsilon_{y,lattice}$	[pm]	0.75	1.25	0.85	0.9
Arc cell		Long 90/90		90/90	
Momentum compaction α_p	[10 ⁻⁶]	28.6		7.4	
Arc sext families		75		146	
$\beta_{x/y}^*$	[mm]	110 / 0.7	220 / 1	240 / 1	1000 / 1.6
Transverse tunes $Q_{x/y}$		218.158 / 222.200	218.186 / 222.220	398.192 / 398.358	398.148 / 398.182
Chromaticities $Q'_{x/y}$		0 / +5	0 / +2	0 / 0	0 / 0
Energy spread (SR/BS) σ_δ	[%]	0.039 / 0.089	0.070 / 0.109	0.104 / 0.143	0.160 / 0.192
Bunch length (SR/BS) σ_z	[mm]	5.60 / 12.7	3.47 / 5.41	3.40 / 4.70	1.81 / 2.17
RF voltage 400/800 MHz	[GV]	0.079 / 0	1.00 / 0	2.08 / 0	2.1 / 9.38
Harm. number for 400 MHz		121200			
RF frequency (400 MHz)	MHz	400.786684			
Synchrotron tune Q_s		0.0288	0.081	0.032	0.091
Long. damping time	[turns]	1158	219	64	18.3
RF acceptance	[%]	1.05	1.15	1.8	2.9
Energy acceptance (DA)	[%]	±1.0	±1.0	±1.6	-2.8/+2.5
Beam crossing angle at IP $\pm\theta_x$	[mrad]	±15			
Piwinski angle $(\theta_x\sigma_{z,BS})/\sigma_x^*$		21.7	3.7	5.4	0.82
Crab waist ratio	[%]	70	55	50	40
Beam-beam ξ_x/ξ_y^a		0.0023 / 0.096	0.013 / 0.128	0.010 / 0.088	0.073 / 0.134
Lifetime (q + BS + lattice)	[sec]	15000	4000	6000	6000
Lifetime (lum) ^b	[sec]	1340	970	840	730
Luminosity / IP	[10 ³⁴ /cm ² s]	140	20	5.0	1.25
Luminosity / IP (CDR, 2 IP)	[10 ³⁴ /cm ² s]	230	28	8.5	1.8

Synchrotron Radiation Spectra

90.7 km machine

Critical energy: $\epsilon_c = 2218 \cdot E^3 \text{ (GeV)} / \rho \text{ (m)}$

- **Z-Pole: very high photon flux (→ large outgassing load);**
- **Z-pole: compliance with scheduled operation (integrated luminosity first 2 years), requires quick commissioning to $I_{\text{NOM}}=1.390 \text{ A}$ 1270 mA;**
- **T-pole (182.5): extremely large and penetrating radiation, critical energy 1.25 MeV 1.36 MeV;**
- **T-pole (and also W and H): need design which minimizes activation of tunnel and machine components (→ FLUKA);**
- **W, H-pole: intermediate between Z and T; still $E_{\text{crit}} >$ Compton edge (~100 keV (Al), ~200 keV (Cu))**

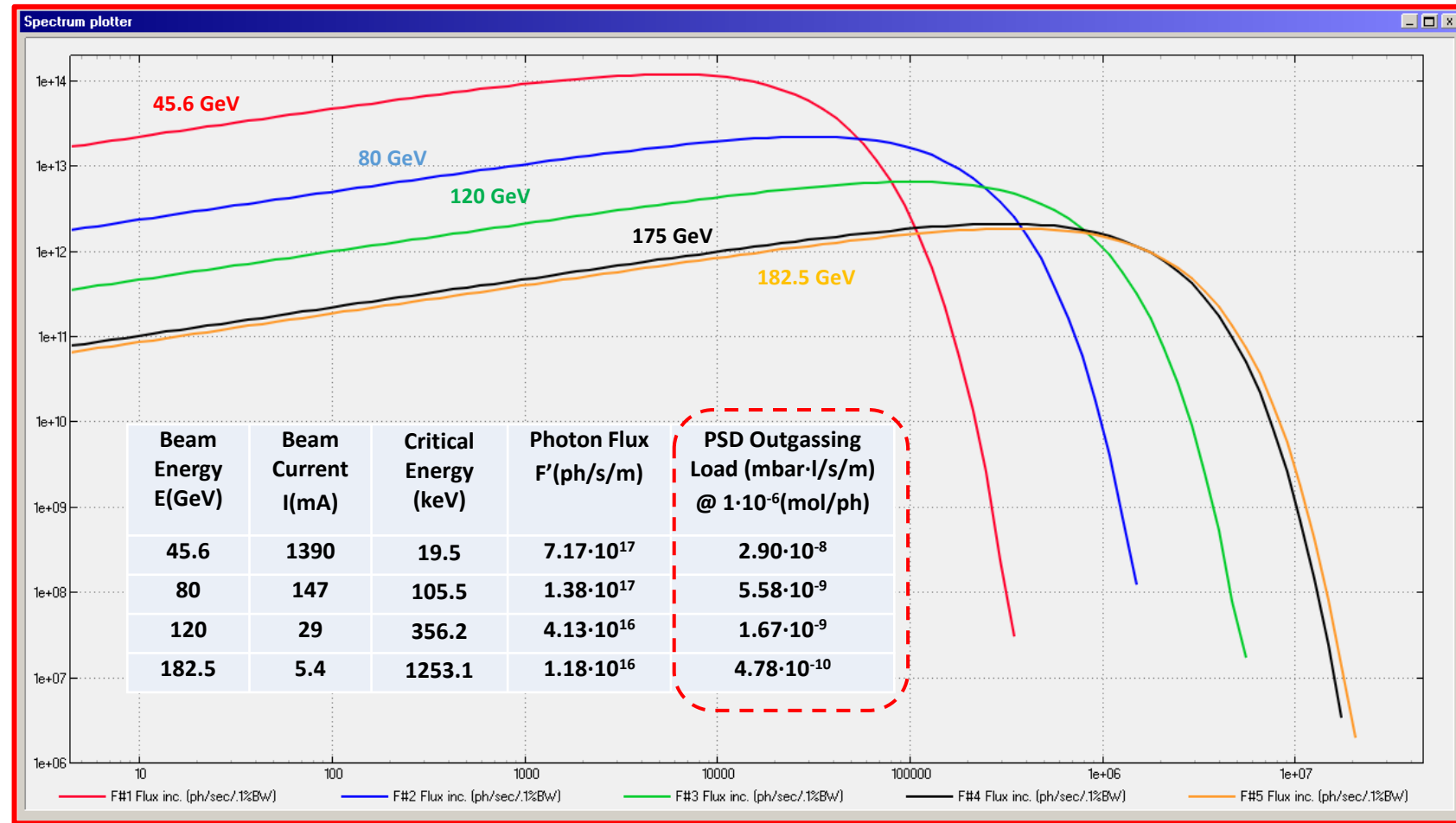
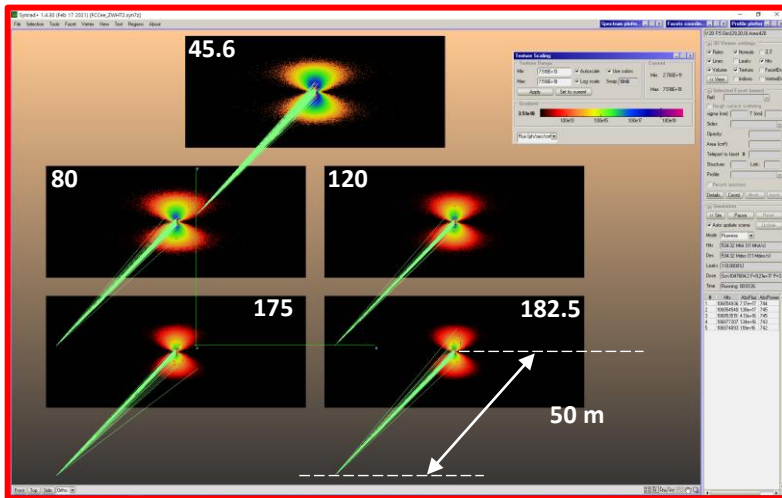


Synchrotron radiation spectrum, flux, power

Typical vertical opening angle SR: $1/\gamma$; $\gamma(\text{ttbar})=357,143$; $1/\gamma=2.8 \mu\text{rad} \rightarrow @50 \text{ m} = 0.14 \text{ mm}$

SR Spectra computed with SYNRAD+

- Radiation projected onto five $14 \times 6 \text{ cm}^2$ screens;
- 1 cm-long dipole arc trajectories;
- Flux distribution shown here,
- Logarithmic scale for textures,
- 6 orders of magnitude displayed;



Units: Vertical: photons/s/(0.1% bandwidth)/m; Range $[10^6 - 2 \cdot 10^{14}]$
Horizontal eV; Range $[4 - 5 \cdot 10^7]$

- Gas Load for W-, H-, T-poles will have a significant contribution proportional to SR power, due to Compton photons (as per LEP operation, ref. *“The pressure and gas composition evolution during the operation of the LEP accelerator at 100 GeV”*, M. J. Jimenez et al., Vacuum 60 (2001) p183-189);

<u>F (FCC-ee)>100 keV (%)</u>	
Z	0.0639
W	9.220
H	28.852
T(175)	47.810
T(182.5)	49.717

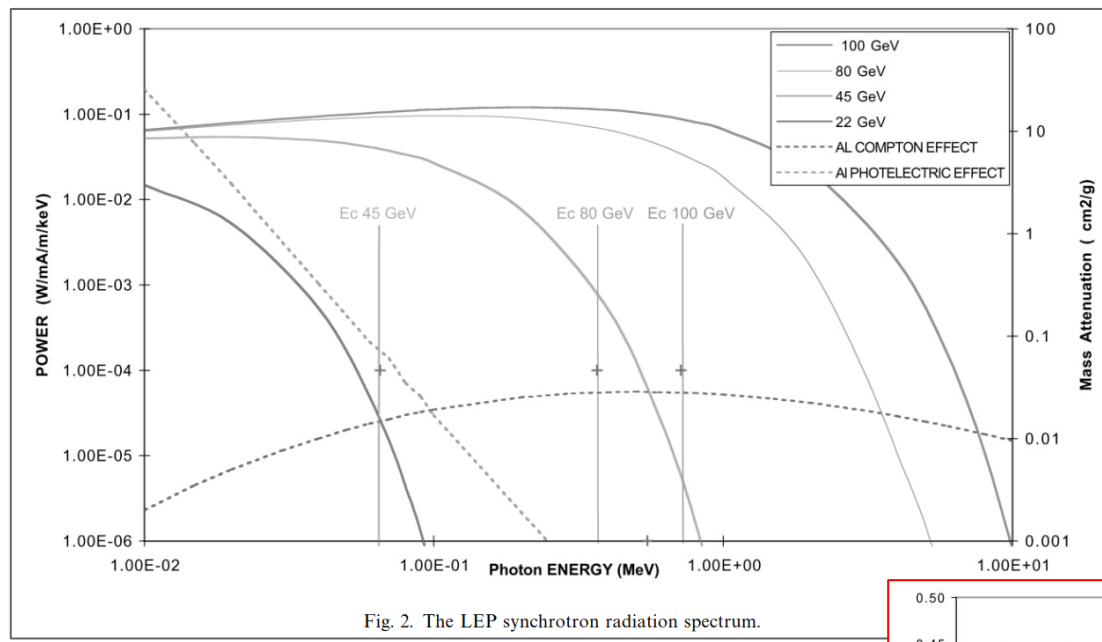


Fig. 2. The LEP synchrotron radiation spectrum.

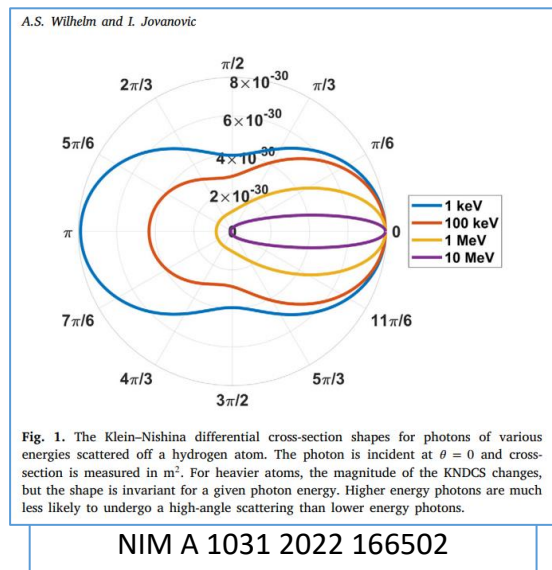


Fig. 1. The Klein-Nishina differential cross-section shapes for photons of various energies scattered off a hydrogen atom. The photon is incident at $\theta = 0$ and cross-section is measured in m^2 . For heavier atoms, the magnitude of the KNDCS changes, but the shape is invariant for a given photon energy. Higher energy photons are much less likely to undergo a high-angle scattering than lower energy photons.

NIM A 1031 2022 166502

- If copper alloy is chosen as the material for the vacuum chamber, then a smaller fraction goes into Compton, and shielding improves;
- In addition, copper has a lower photon-stimulated desorption yield;

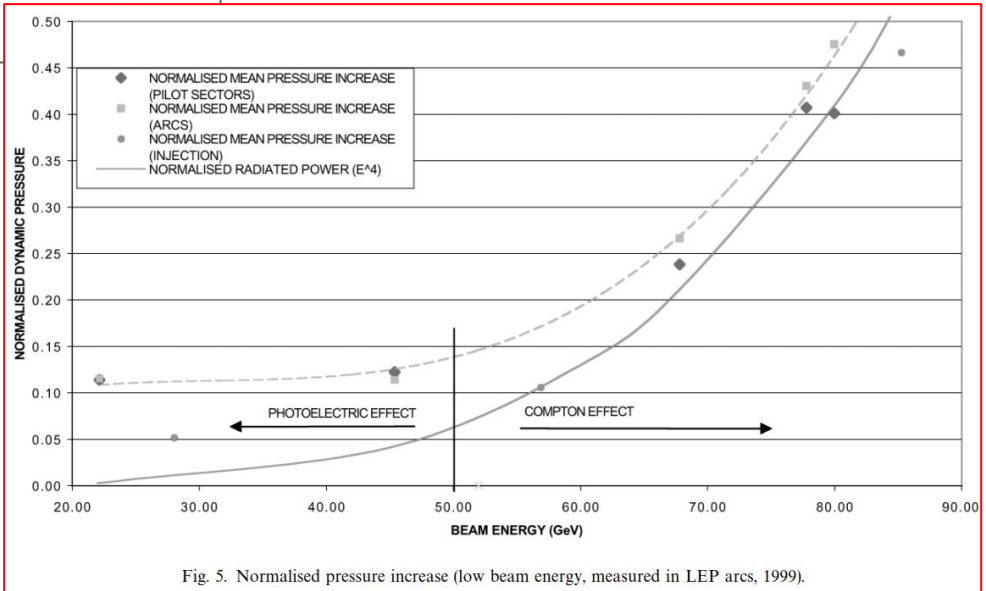
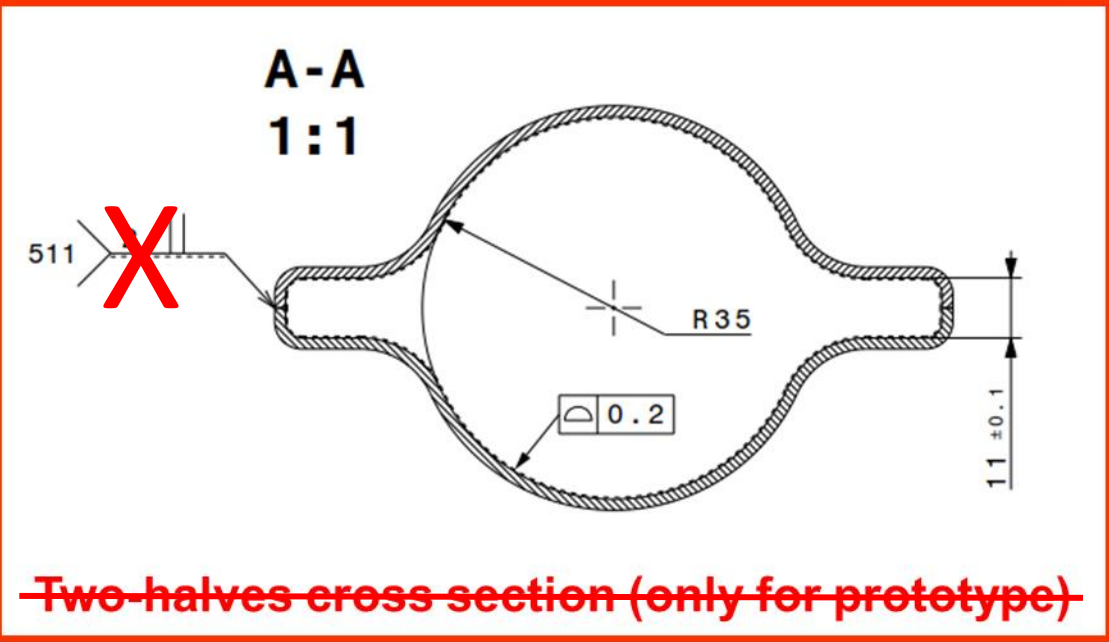
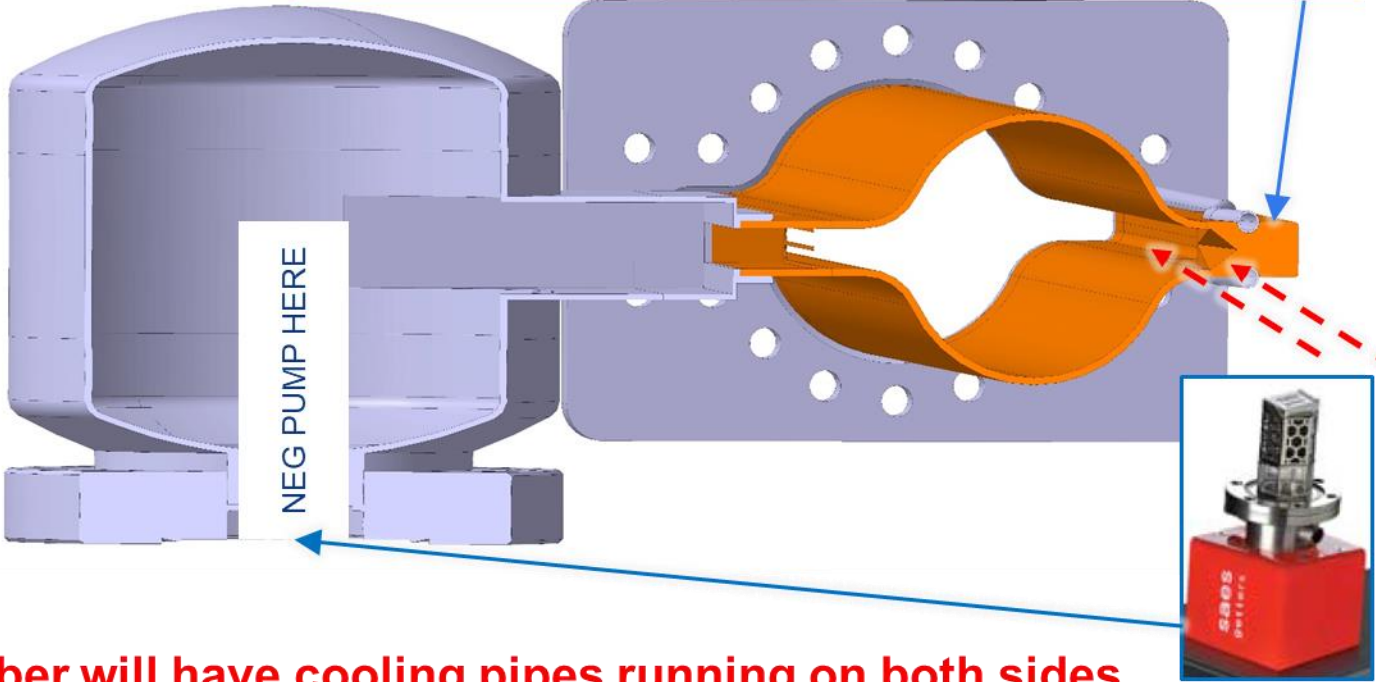


Fig. 5. Normalised pressure increase (low beam energy, measured in LEP arcs, 1999).

Material: OFC copper; Specific Cond.: 48.2 l·m/s (CO, 20 °C)



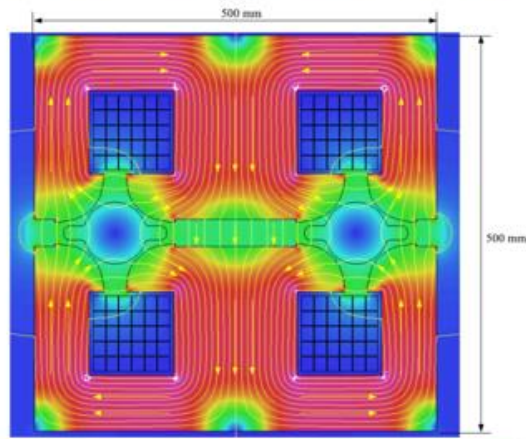
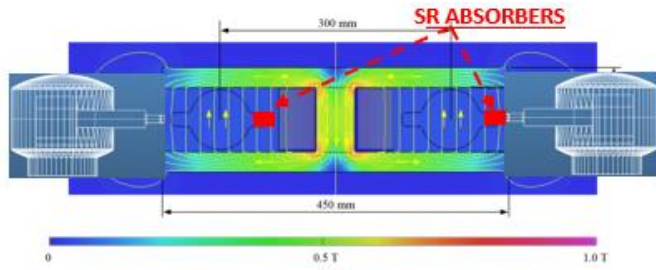
Lumped absorbers (1 every ~ 6 m, covering the entire horizontal SR photon fan)



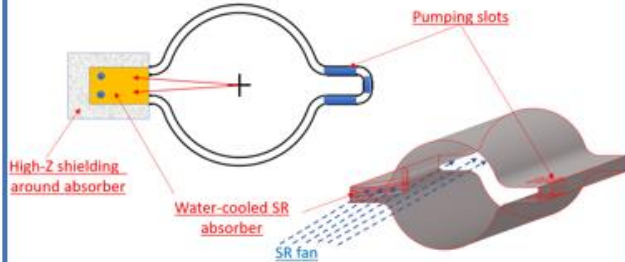
- Left: Cross-section of the prototype (real chamber will have cooling pipes running on both sides of winglets);
- Right: Cross-section at pumping dome/absorber location; The connection to the beam chamber is via a slotted grid; The SR absorber is placed in front of the pumping dome (for external beam only); The conductance of the pumping dome and tapered transition is ~ 110 l/s (CO, 20 C);

We have been asked to look at the possibility to use a smaller vacuum chamber, with internal radius of 30 mm instead of 35: under study now, seems feasible, although the specific conductance decreases to ~30 l·m/s

Pumping solutions: NEG-coating everywhere + lumped NEG pumps

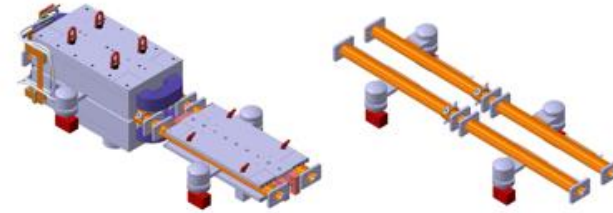
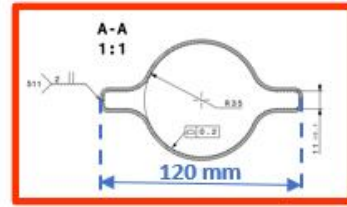


Material: OFC copper;
Specific Cond.: ~ 47 l·m/s (CO, 20 °C)

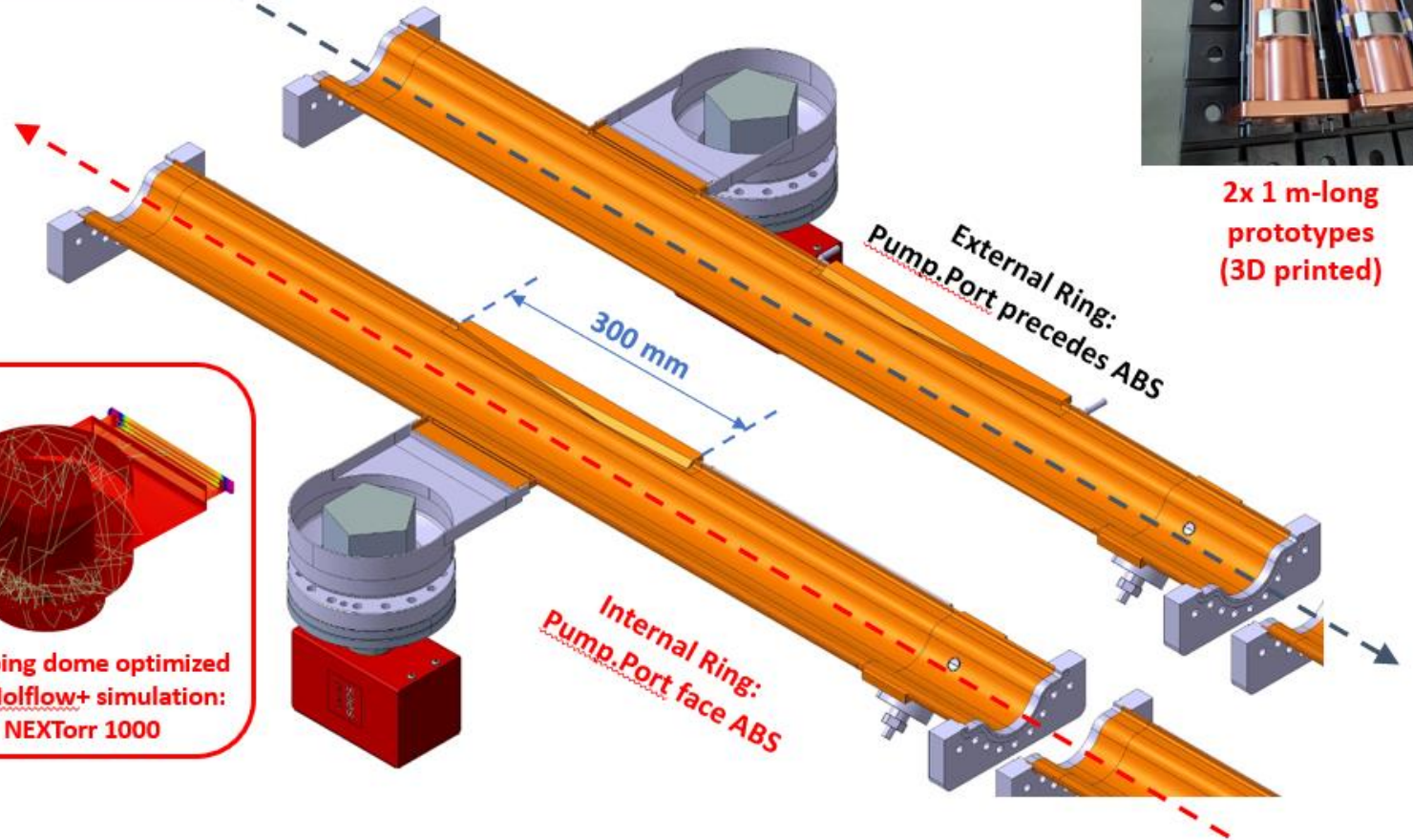


Schematics of SR absorbers and pumping slots (internal beam)

FCC-ee CAD Models

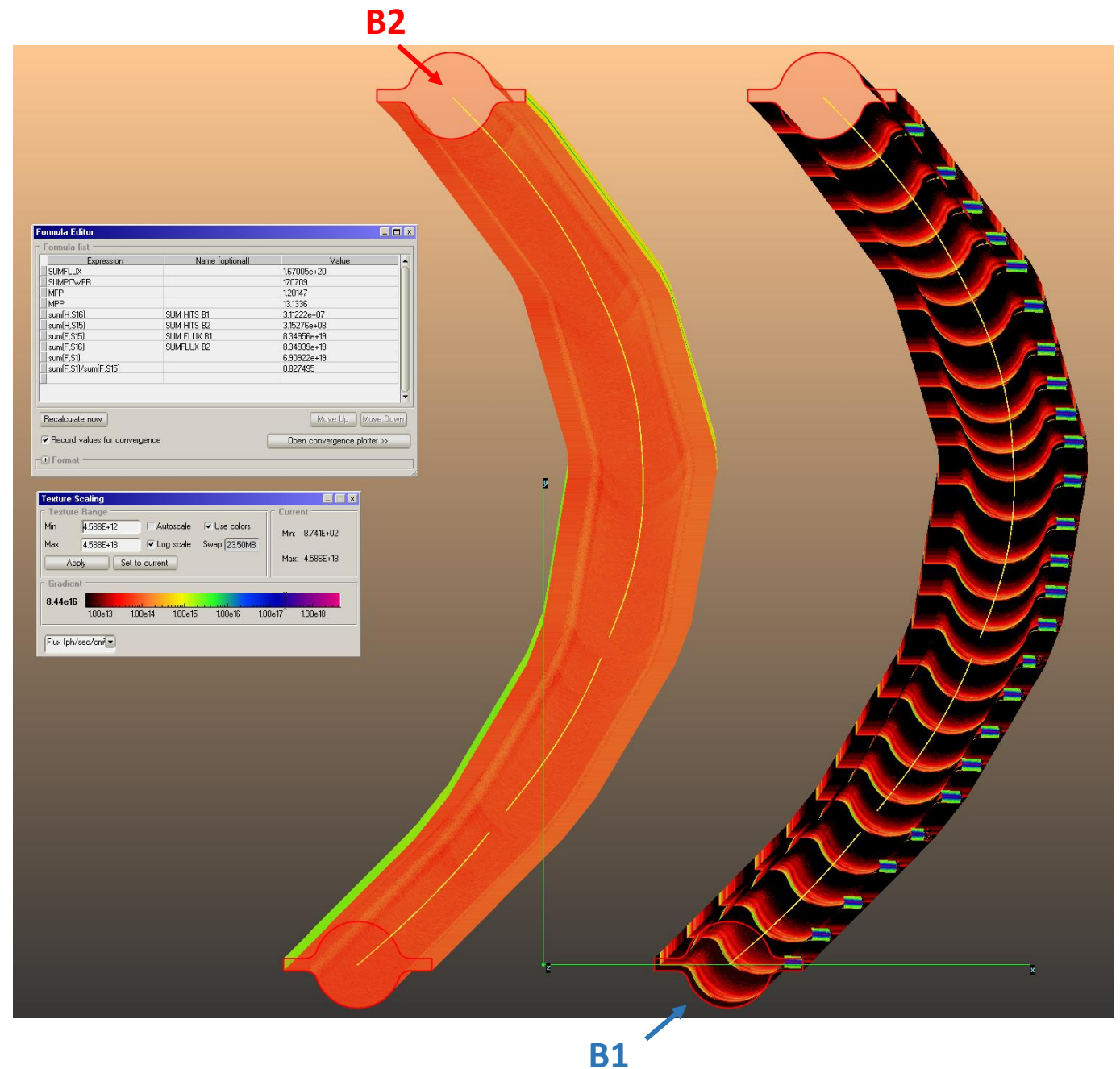


2x 1 m-long prototypes (3D printed)



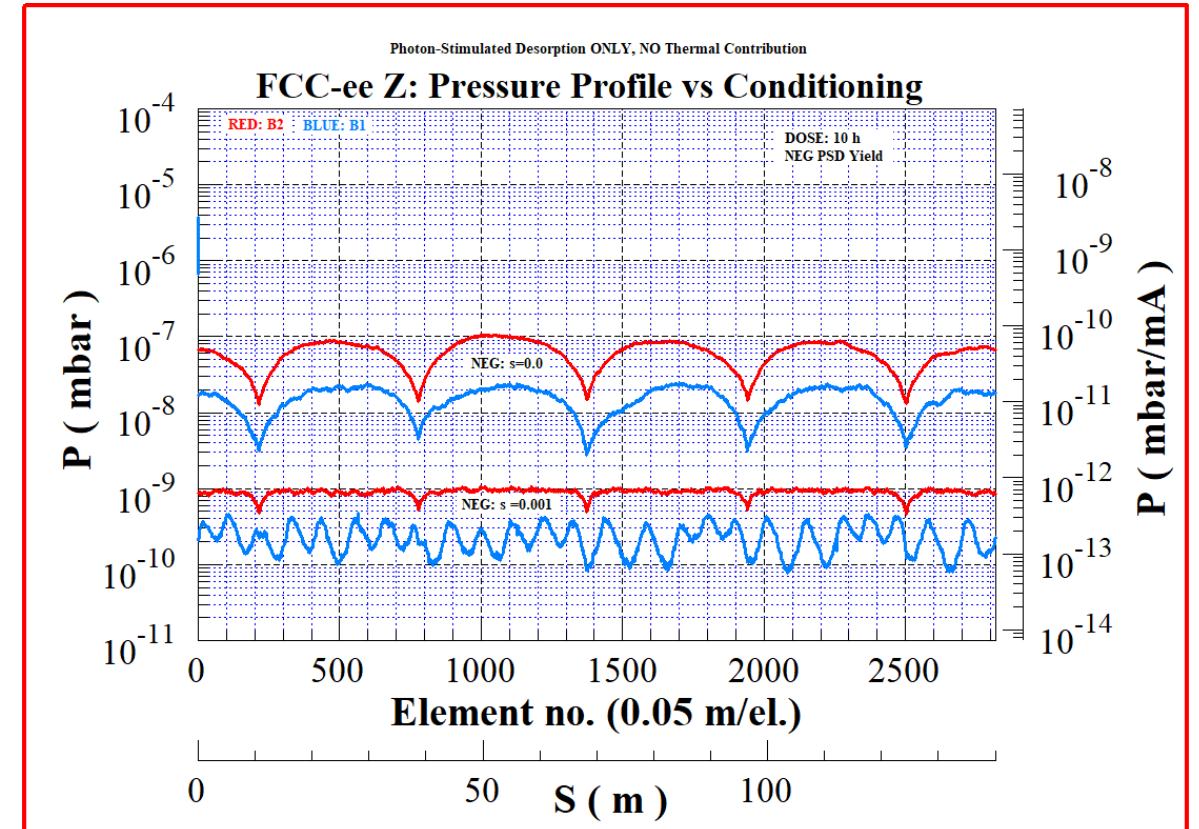
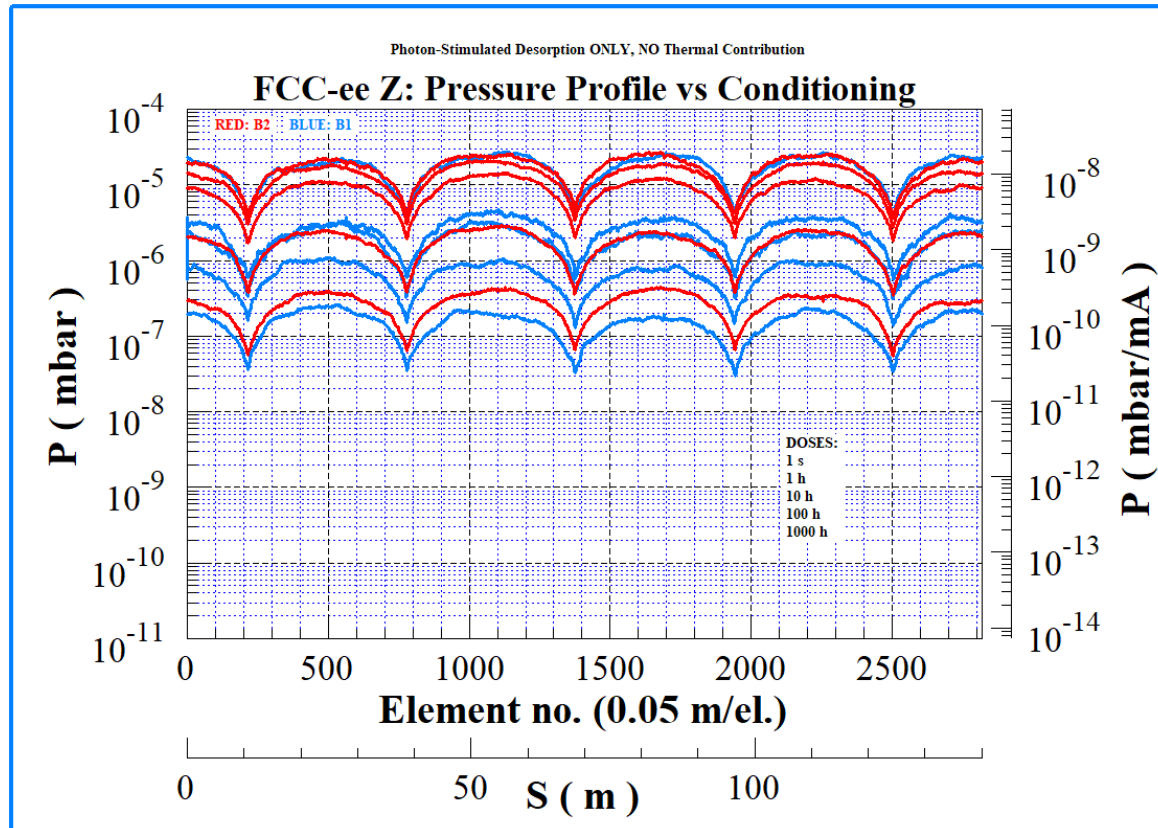
Pressure profiles

- These 2 models represent a section of the arcs (~140 m long)
- We have used Molflow+ to calculate the PSD pressure rise at different beam doses, using the photon irradiation maps calculated by SYNRAD+
- A sample 140.7 m-long section of an arc has been considered, with the two beams side by side: 5 dipoles and 5 quadrupoles as sources of SR
- The orbits along 5 dipoles interleaved with 5 quadrupoles are simulated, importing the lattice files from MADX into SYNRAD+
- The 3D model for B1 has 25 absorbers placed at ~ 5.6 m average spacing (avoiding quadrupoles and sextupoles which have tight coils), while B2 has no absorbers, and the SR fan is let impinge onto the bottom of the external winglet (see also B. Humann, FCC Week)
- The MDI region adopts the same philosophy: **lumped absorbers covering ~100% of the primary SR photon fans**



Pressure profiles

- We have calculated the PSD pressure profiles for 5 different beam doses, corresponding to times of 1 s, 1 h, 10 h, 100 h, 1000 h. Simulated gas: CO
- On the left the case with 5x 100 (l/s) lumped pumps/beam, and no NEG-coating
- On the right, the case with NEG-coating, saturated (i.e $s=0$) and with some residual sticking ($s=0.001$)



MDI Interaction Point: sources of radiation and radiation dump

SOURCE

- SR EM-fields of colliding bunches (Beamstrahlung)
- SR solenoid (2T) + anti-solenoid
- SR IR quadrupoles
- radiative Bhabha (beam-beam Bremsstrahlung)

POWER

- ~ 400 kW
- ~ 40 kW
- ~ 7 kW
- ~ 0.7 kW

CRITICAL ENERGY

- ~ 2 MeV
- ~ 0.02 MeV
- ~ 0.02 MeV
- ~ 5000 MeV

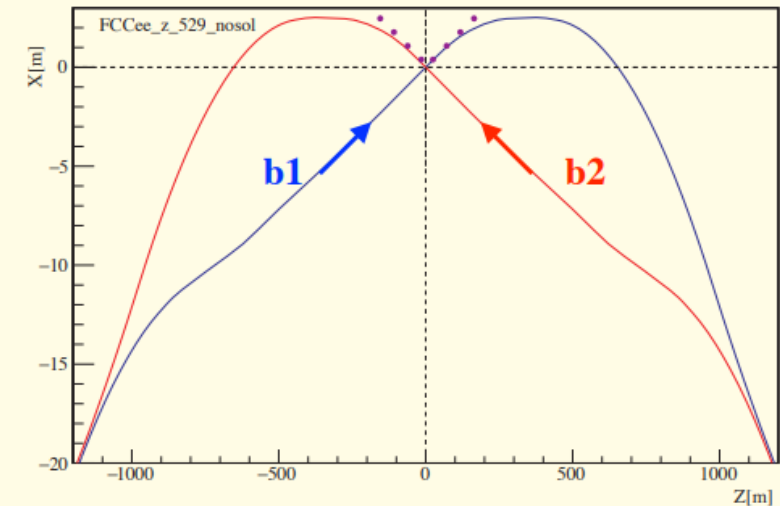
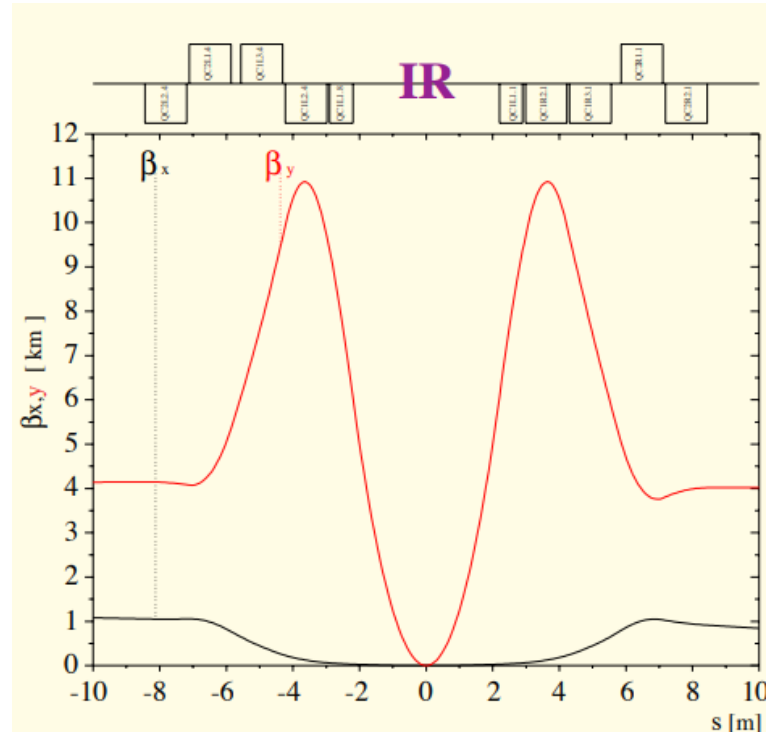
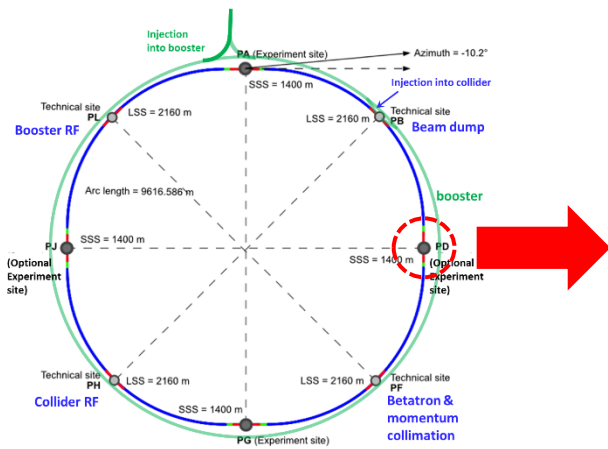
8th FCC-ee Physics Workshop - Paris - 4. November 2014

$$e f k N = \text{beam current} \propto \frac{1}{E^3}$$

$$L = \frac{f k N^2}{4\pi\sigma_x\sigma_y} F H$$

$\xi_y \propto \frac{\beta_y^* N}{E\sigma_x\sigma_y} \leq \xi_y^{\max}(E)$ Beam-beam parameter

$$L \propto \frac{P_{SR}}{E^3} \frac{\xi_y}{\beta_y^*}$$



Beta functions and geometry of the IP region; crossing angle is 30 mrad

MDI Interaction Point: sources of radiation and radiation dump

- **Main goal:** reduce/eliminate the radiation background reaching the detector
- Five main effects (excluding hot-spots and heating due to impedance issues)

FCC Brainstorming on Beamstrahlung radiation handling 08/03/2022 **Andrea Ciarna** 3

Beamstrahlung

Beamstrahlung photons have been generated using **GuineaPig++**.

$\langle E_\gamma \rangle =$
 67MeV @ \bar{I}
 23MeV @ ZH
 10MeV @ WW
 2MeV @ Z

The photon beam divergence is similar for x and y at all energies (~50 μ rad), so the beam spot will be round. As an example @50m from the IP the spot would be about 1x1cm²

The photon angular emission is **proportional to the vertical offset** between the two beams for small offsets, while it saturates when the beams are several sigmas apart.

FCC Brainstorming on Beamstrahlung radiation handling 08/03/2022 **Andrea Ciarna** 4

Radiative Bhabha

BBBrem generates single photon events considering head-on on-axis collisions.

These events are used as inputs in **GuineaPig++** them in the correct frame (considering also smear them along the nominal particles direction step-by-step tracking).

Also in this depends between t Radiative lower flux but the photon higher energy

Radiative Bhabha at zero photon scattering angle

FCC Brainstorming on Beamstrahlung radiation handling 08/03/2022 **Andrea Ciarna** 6

Backgrounds: Compton Scattering on Thermal Photons

Thermal photons can gain energy via Compton scattering with the electrons of the beam, according to

$$\frac{d\sigma}{dy} = \frac{2\sigma_0}{x} \left[\frac{1}{1-y} + 1-y - \frac{4y}{x(1-y)} \left(1 - \frac{y}{x(1-y)} \right) \right] \quad x = \frac{4E\omega\gamma\cos^2(\alpha/2)}{(mc^2)^2}$$

V.I. Telnov - NIM A260 (1987) 304-308
 D. Burkhardt - SL/7609 93-23-1407
 y = ω'/E

The photon flux coming from this source has been simulated using a custom generator considering a temperature of 300K.

This photons are emitted in the direction of the beam and can reach energies **up to few GeV**, so this might constitute a source of background for the Radiative Bhabhas.

FCC Brainstorming on Beamstrahlung radiation handling 08/03/2022 **Andrea Ciarna** 7

Backgrounds: Inelastic Beam Gas Scattering

Also the Bremsstrahlung radiation produced by the **inelastic scattering** of the beam particles with **residual gas** in the beam pipe constitutes an unavoidable source of background for this monitor.

$$\frac{d\sigma}{dy} = \frac{16\alpha r_e^2}{3} Z(Z+1) \frac{1}{y} (1-y-0.75y^2) \log\left(\frac{184.15}{Z^{1/3}}\right)$$

This radiation can reach up to the nominal beam energy, falling therefore in the same range of the radiative bhabha emissions.

FCC Brainstorming on Beamstrahlung radiation handling 08/03/2022 **Andrea Ciarna** 5

Backgrounds: Synchrotron Radiation

Synchrotron radiation produced by the **final focusing quadrupoles** constitutes a background source for this detector.

SYNRAD+ has been used to simulate the flux through a 1x1cm² facet orthogonal to the photon beam axis placed 50m downstream. The dominant contribution to this radiation comes from the innermost final focusing quadrupoles.

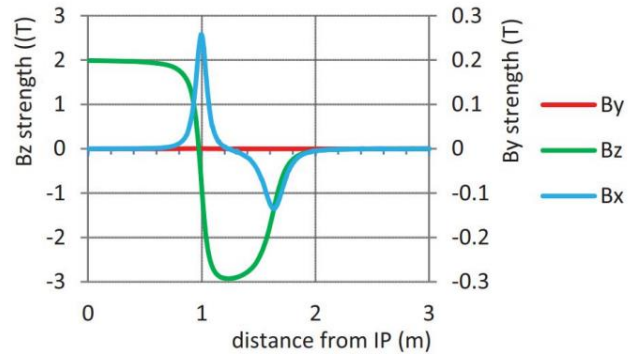
	Flux [10 ¹⁸ ph/sec]	Power [kW]
Total	2.31	2.57
QC1L	1.04	1.22
QC1R	1.12	1.33
QC2L	0.06	0.01
QC2R	0.09	0.01

MDI Interaction Point: sources of radiation and radiation dump

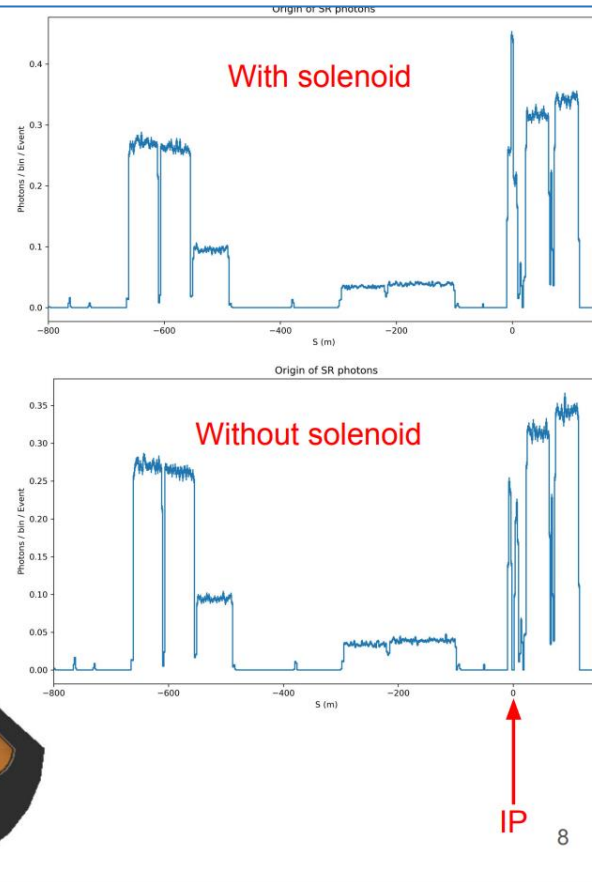
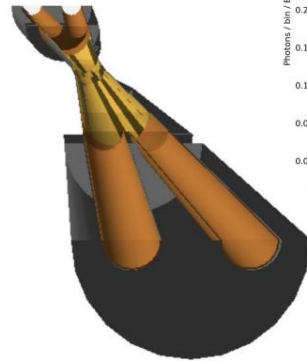
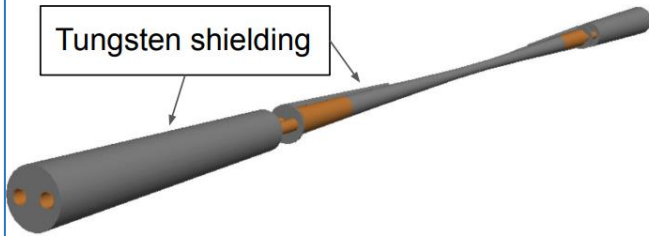
- Solenoid/anti-solenoid fields (K.D.J. André); Strong effect on SR
- 2T @ 15 mrad

Central beam pipe & 3D field map

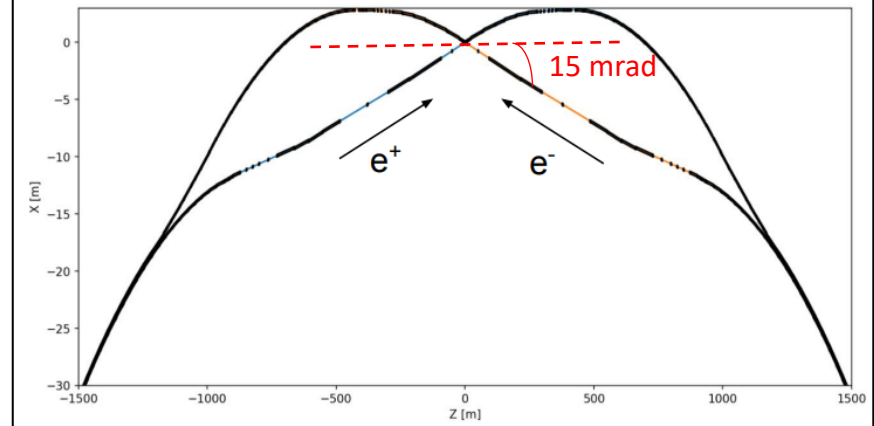
magnetic field along electron path



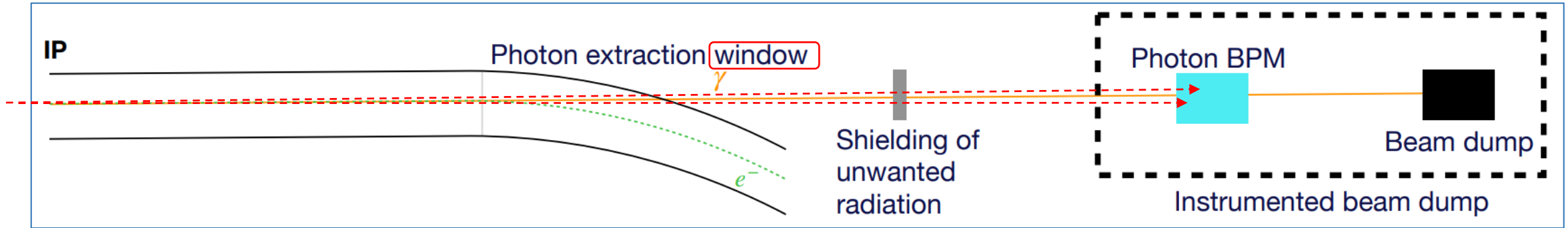
Tungsten shielding



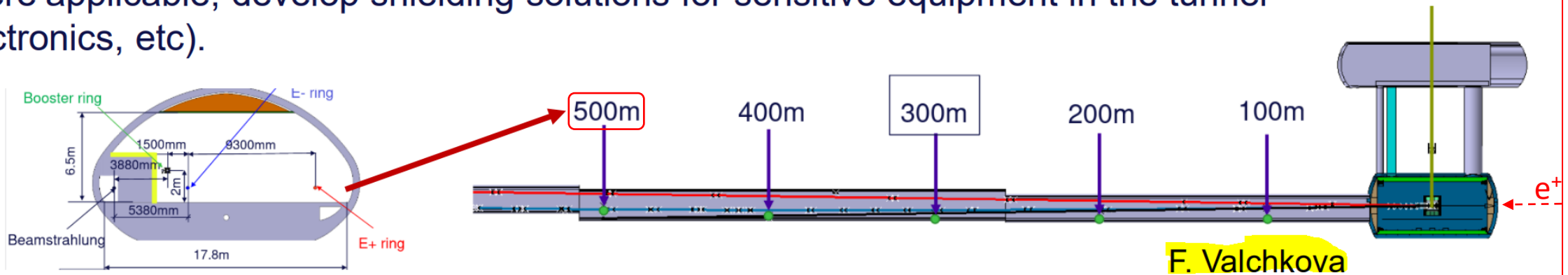
The lattice around the IP



MDI Interaction Point: sources of radiation and radiation dump

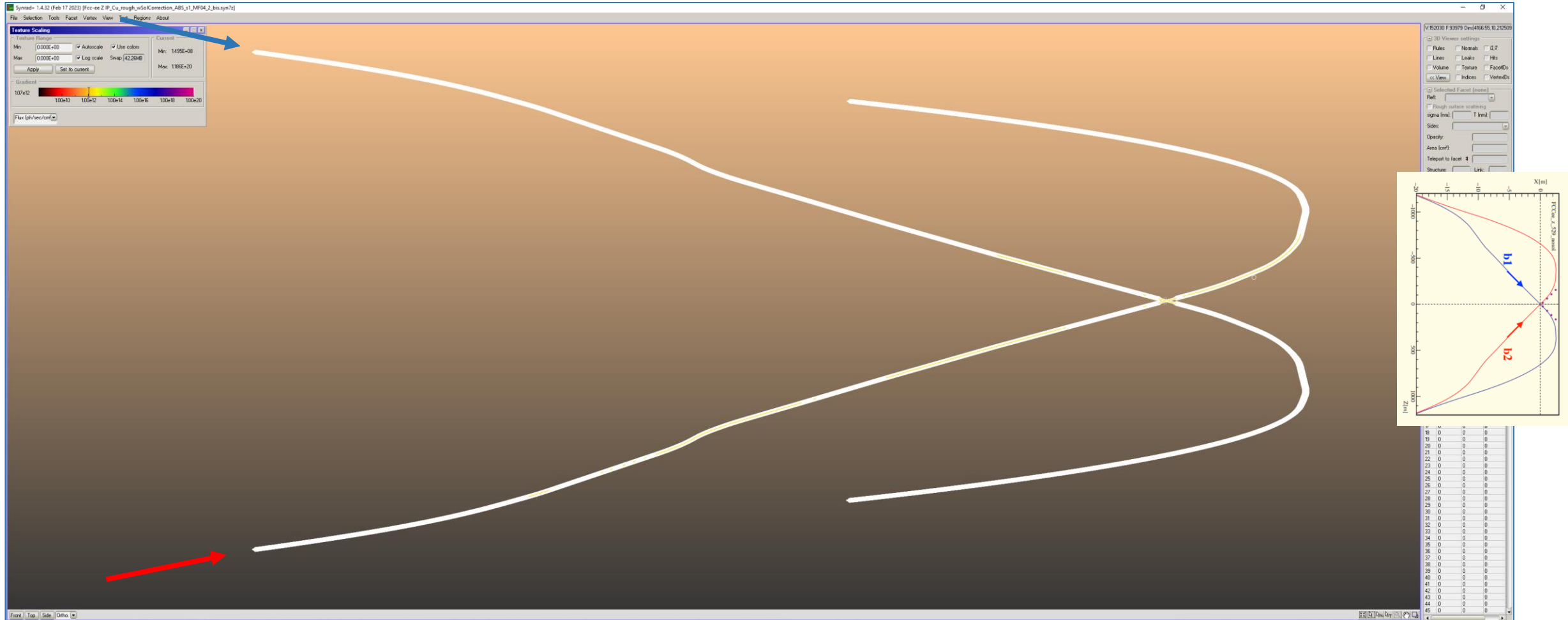
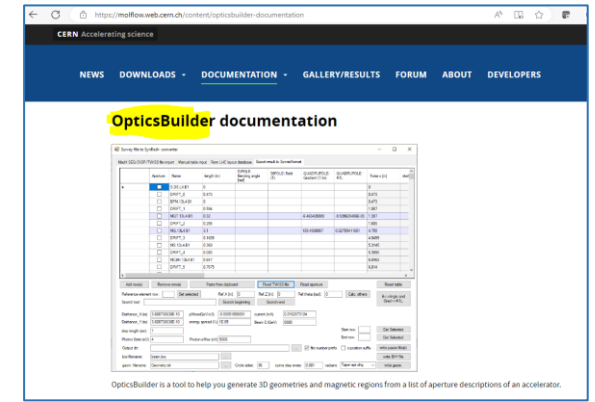


- Where applicable, develop shielding solutions for sensitive equipment in the tunnel (electronics, etc).

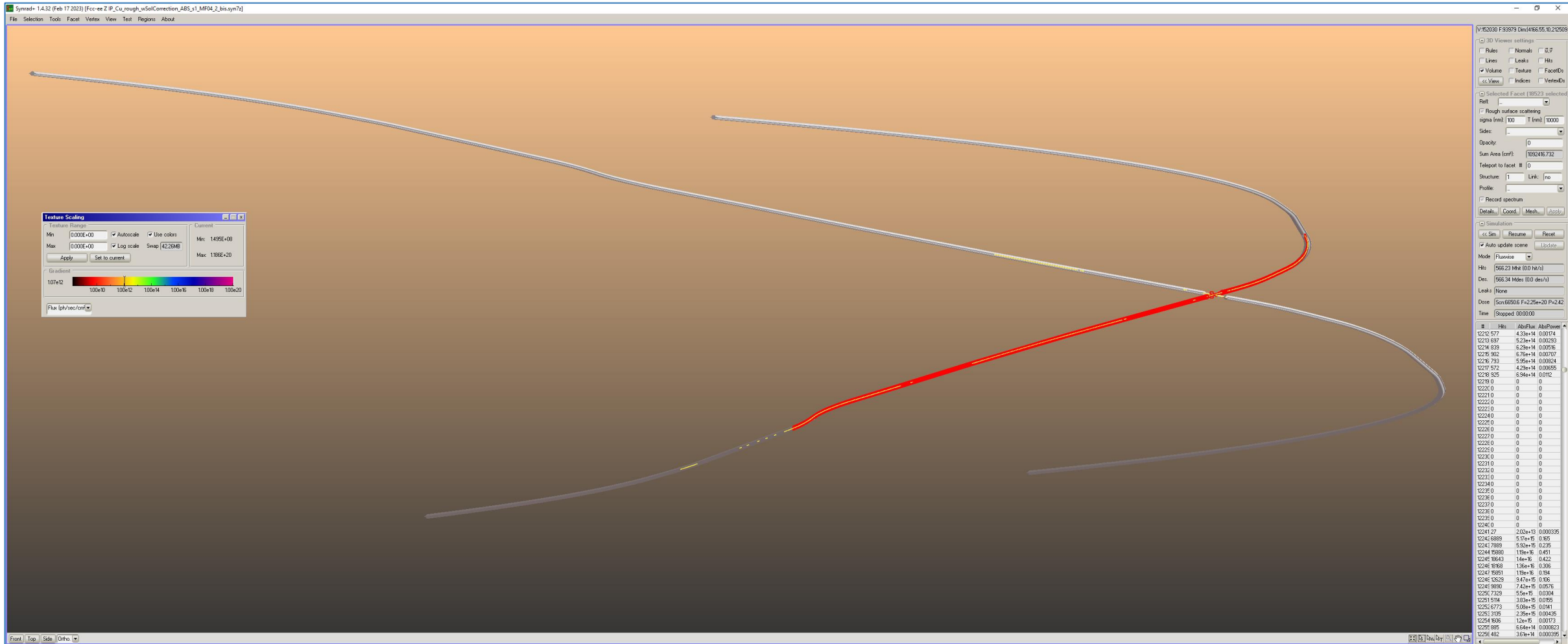


MDI modeling with SYNRAD+ and Molflow+:

Model created automatically from the lattice files (M. Ady, via OpticsBuilder)
Crossing angle is $30 \text{ mrad} = 1.72^\circ$



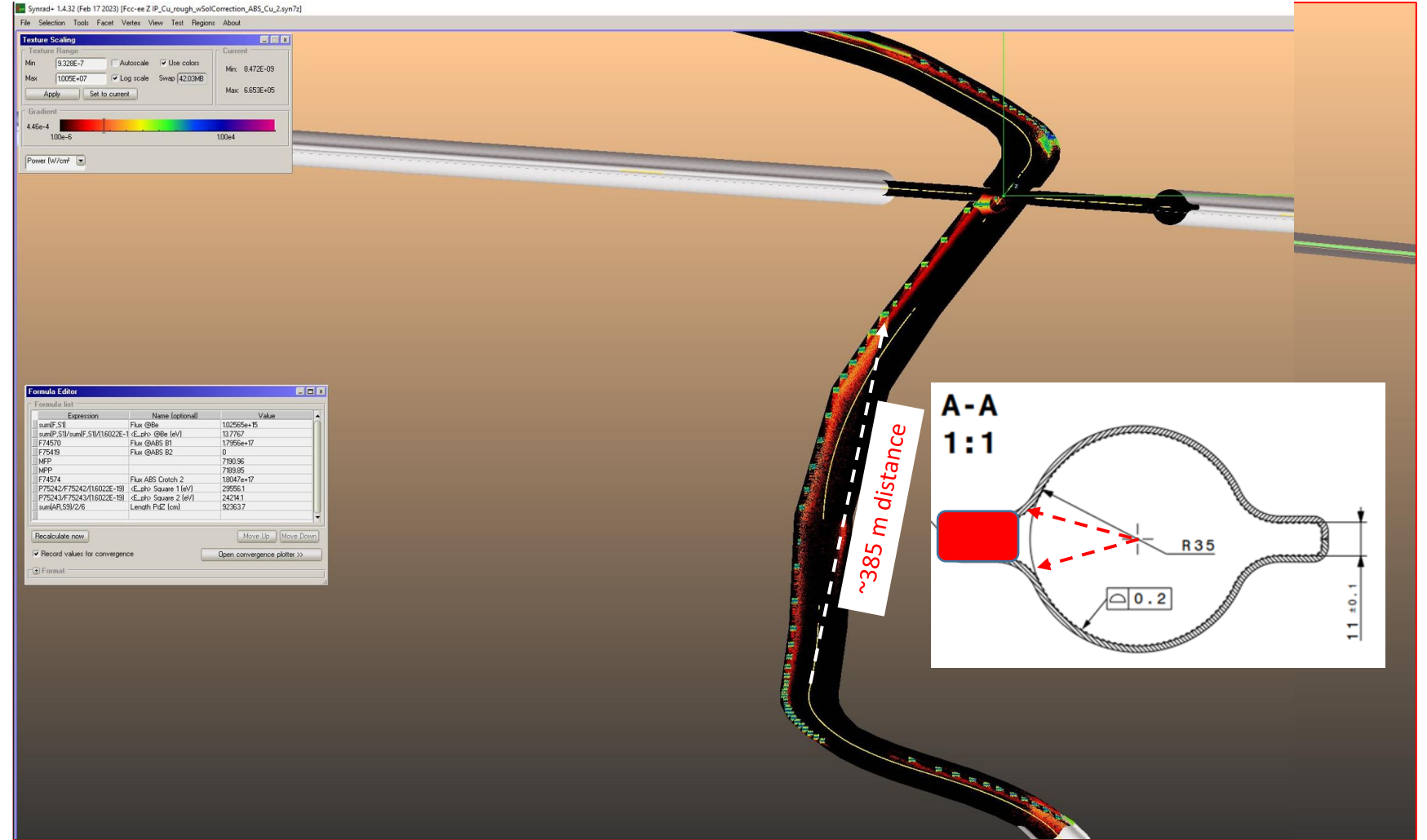
Full length of the model is 2x 1902 m; only the part in red has been modeled, 923 m long (incoming beam, left to right)



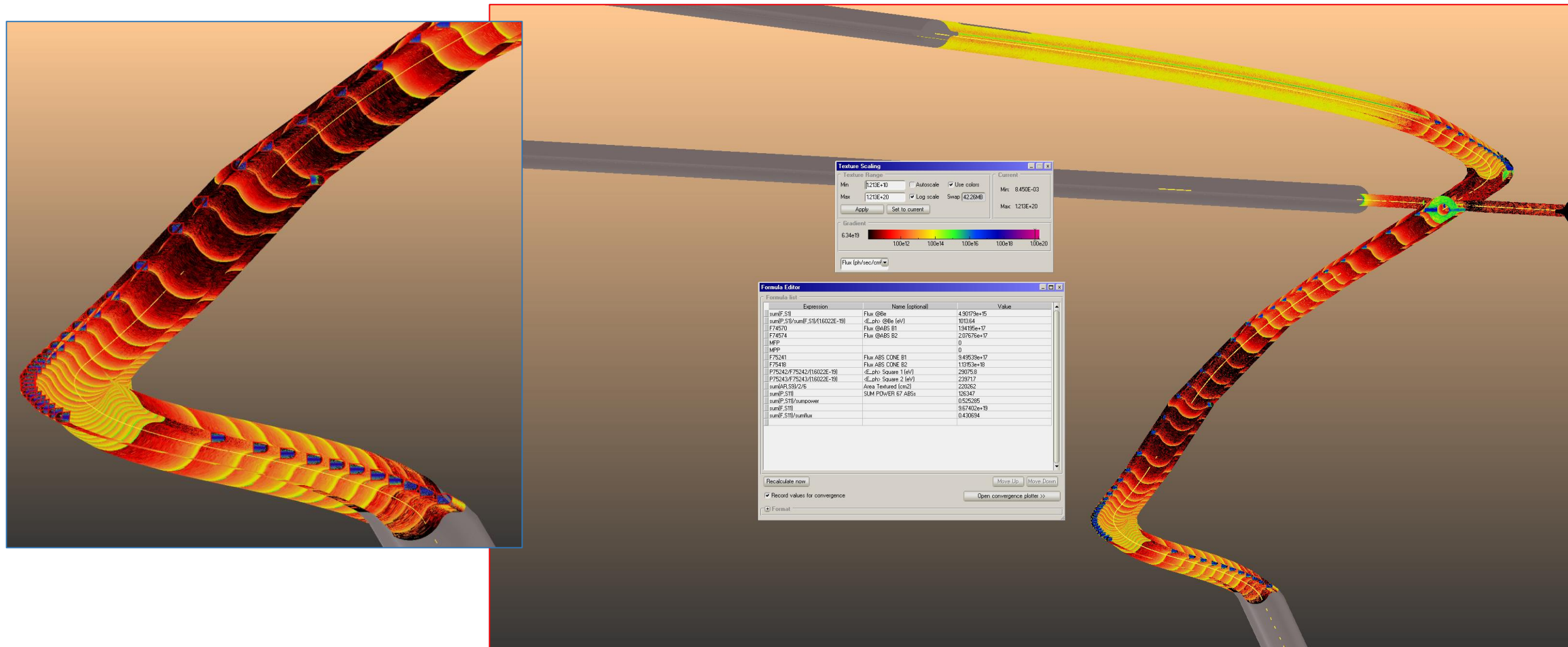
There are a total of 64 magnetic “regions” (in SYNRAD+ parlance) considered, comprising dipoles, quadrupoles, and the solenoid/antisolenoid combination inside the detector (see below)

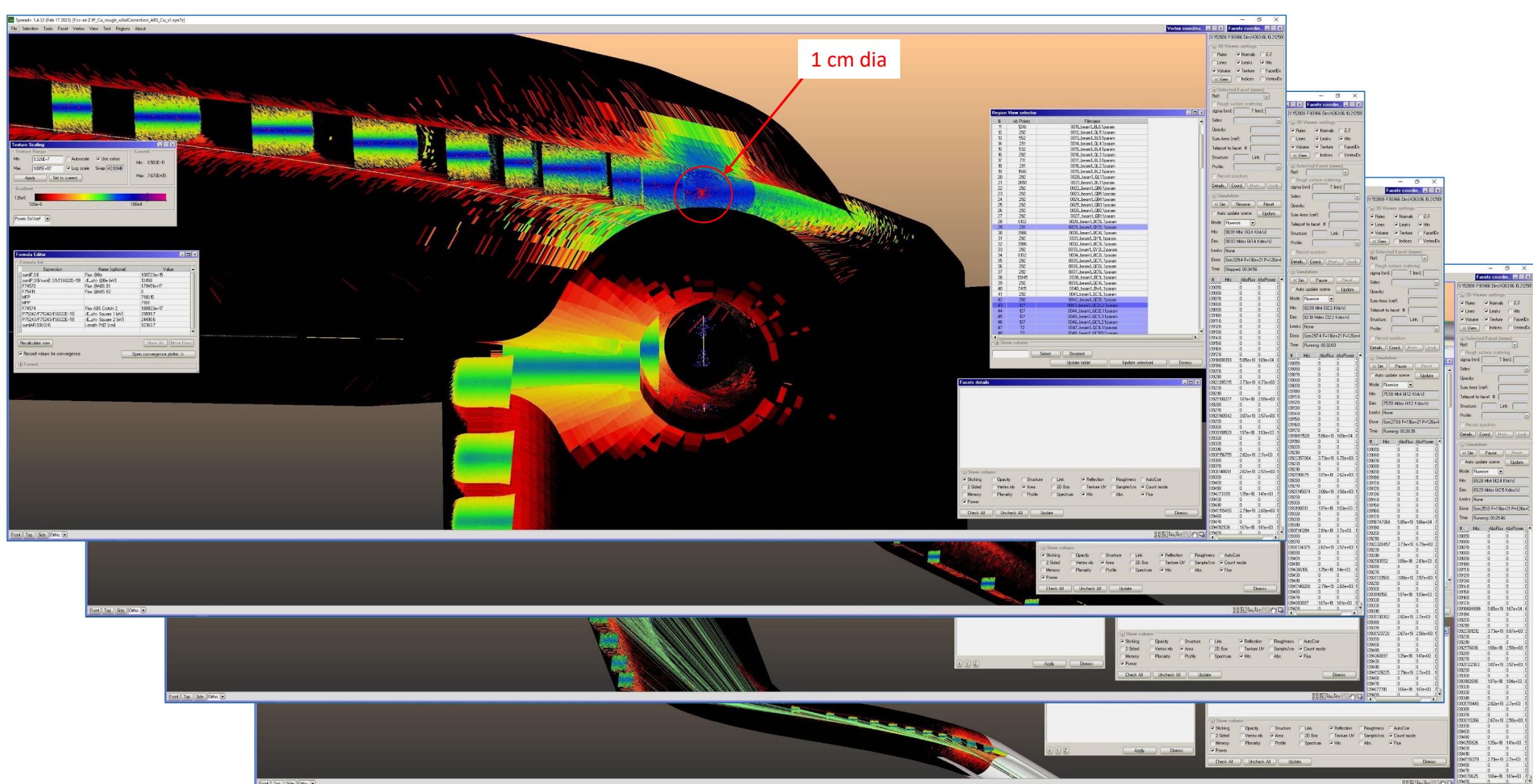
#	nb Points	Filename
1	2650	0021_beamL.BL11.param
2	292	0022_beamL.QB6.1.param
3	292	0023_beamL.QB5.1.param
4	292	0024_beamL.QB4.1.param
5	292	0025_beamL.QB3.1.param
6	292	0026_beamL.QB2.1.param
7	292	0027_beamL.QB1.1.param
8	6102	0028_beamL.BC5L.1.param
9	291	0029_beamL.QY2L.1.param
10	3986	0030_beamL.BC4L.1.param
11	292	0031_beamL.QY1L.1.param
12	3986	0032_beamL.BC3L.1.param
13	292	0033_beamL.QY2L.2.param
14	6102	0034_beamL.BC2L.1.param
15	292	0035_beamL.QC7L.1.param
16	292	0036_beamL.QC6L.1.param
17	292	0037_beamL.QC5L.1.param
18	12845	0038_beamL.BC1L.1.param
19	292	0039_beamL.QC4L.1.param
20	7415	0040_beamL.BWL.1.param
21	292	0041_beamL.QC3L.1.param
22	292	0042_beamL.QC0L.1.param
23	127	0043_beamL.QC2L.2.param
24	127	0044_beamL.QC2L.1.param
25	127	0045_beamL.QC1L.3.param
26	127	0046_beamL.QC1L.2.param
27	72	0047_beamL.QC1L.1.param
28	72	0048_beamL.QC1R1.2.param
29	127	0049_beamL.QC1R2.2.param
30	127	0050_beamL.QC1R3.2.param
31	127	0051_beamL.QC2R1.2.param
32	127	0052_beamL.QC2R2.2.param
33	291	0053_beamL.QC0.2.param
34	292	0054_beamL.QC3.2.param
35	292	0055_beamL.QC4.2.param
36	5637	0056_beamL.BC12.param
37	291	0057_beamL.QC5.2.param
38	668	0058_beamL.BC2.2.param
39	292	0059_beamL.QC6.2.param
40	2466	0060_beamL.BC3.2.param
41	292	0061_beamL.QC7.2.param
42	3127	0062_beamL.BC4.2.param
43	292	0063_beamL.QY2.3.param
44	4035	0064_beamL.BC5.2.param
45	291	0065_beamL.QY12.param
46	4035	0066_beamL.BC6.2.param
47	291	0067_beamL.QY2.4.param
48	3127	0068_beamL.BC7.2.param
49	292	0069_beamL.QA12.param
50	7415	0040_beam2.BWL.3.param
51	292	0041_beam2.QC3L.3.param
52	292	0042_beam2.QC0L.3.param
53	126	0043_beam2.QC2L.3.param
54	126	0044_beam2.QC1L.3.param
55	126	0045_beam2.QC1L.3.param
56	126	0046_beam2.QC1L.2.3.param
57	702	0047_beam2.QC1L.3.param
58	72	0048_beam2.QC1R1.4.param
59	126	0049_beam2.QC1R2.4.param
60	126	0050_beam2.QC1R3.4.param
61	126	0051_beam2.QC2R1.4.param
62	126	0052_beam2.QC2R2.4.param
63	292	0053_beam2.QC0.4.param
64	446	FCCee_MDLAndre.param

- There are a total of 64 magnetic “regions: 49 for B1, 14 for B2, and 1 for the solenoids
- Total power generated by all is **242 kW**; total photon flux is **$2.25 \cdot 10^{20}$ ph/s**
- This is the ray-tracing for the **ideal case of no photon reflection**

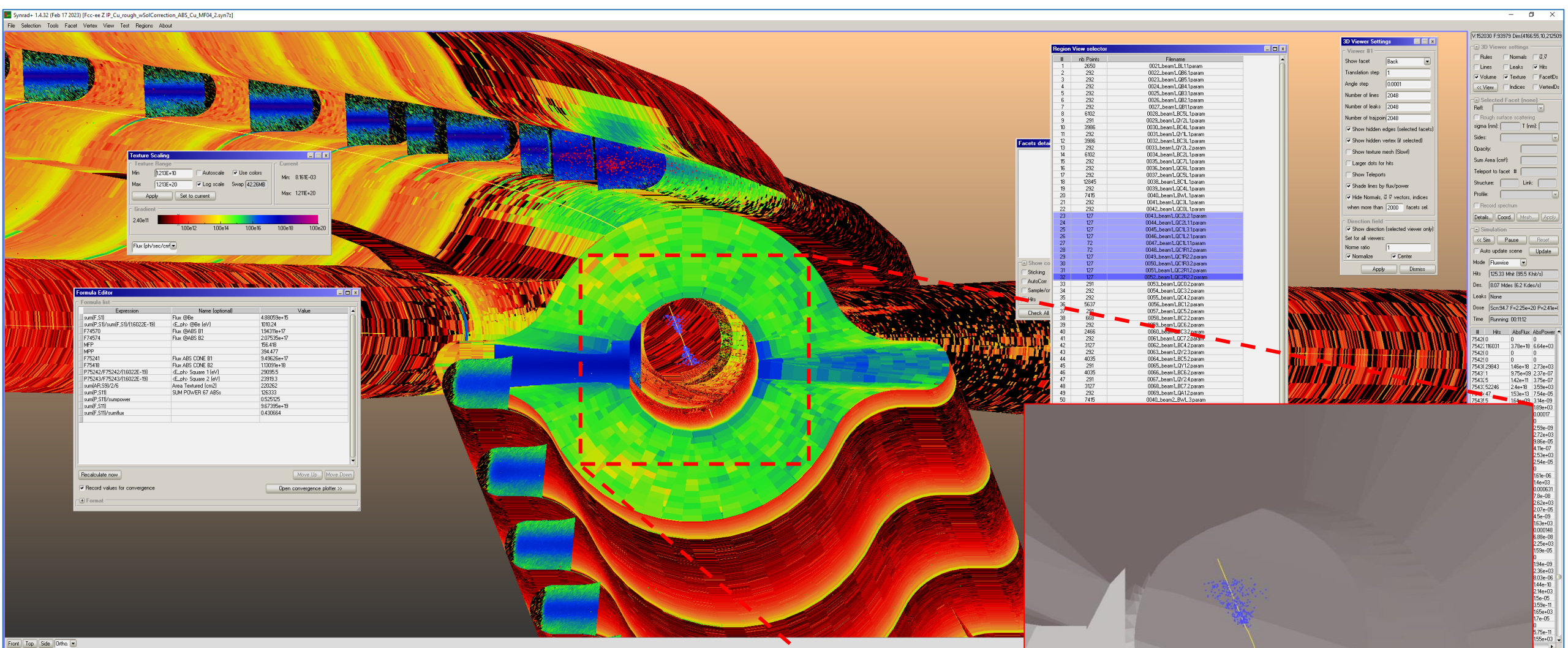


- Here what happens when **angle- and energy-dependent photon reflection** is simulated (with **roughness of the surface taken into account too**)
- **100% of the internal surface of the vacuum chambers** is hit by some photons, whether direct ones or reflected; the consequence is a **SLOWER vacuum conditioning rate**



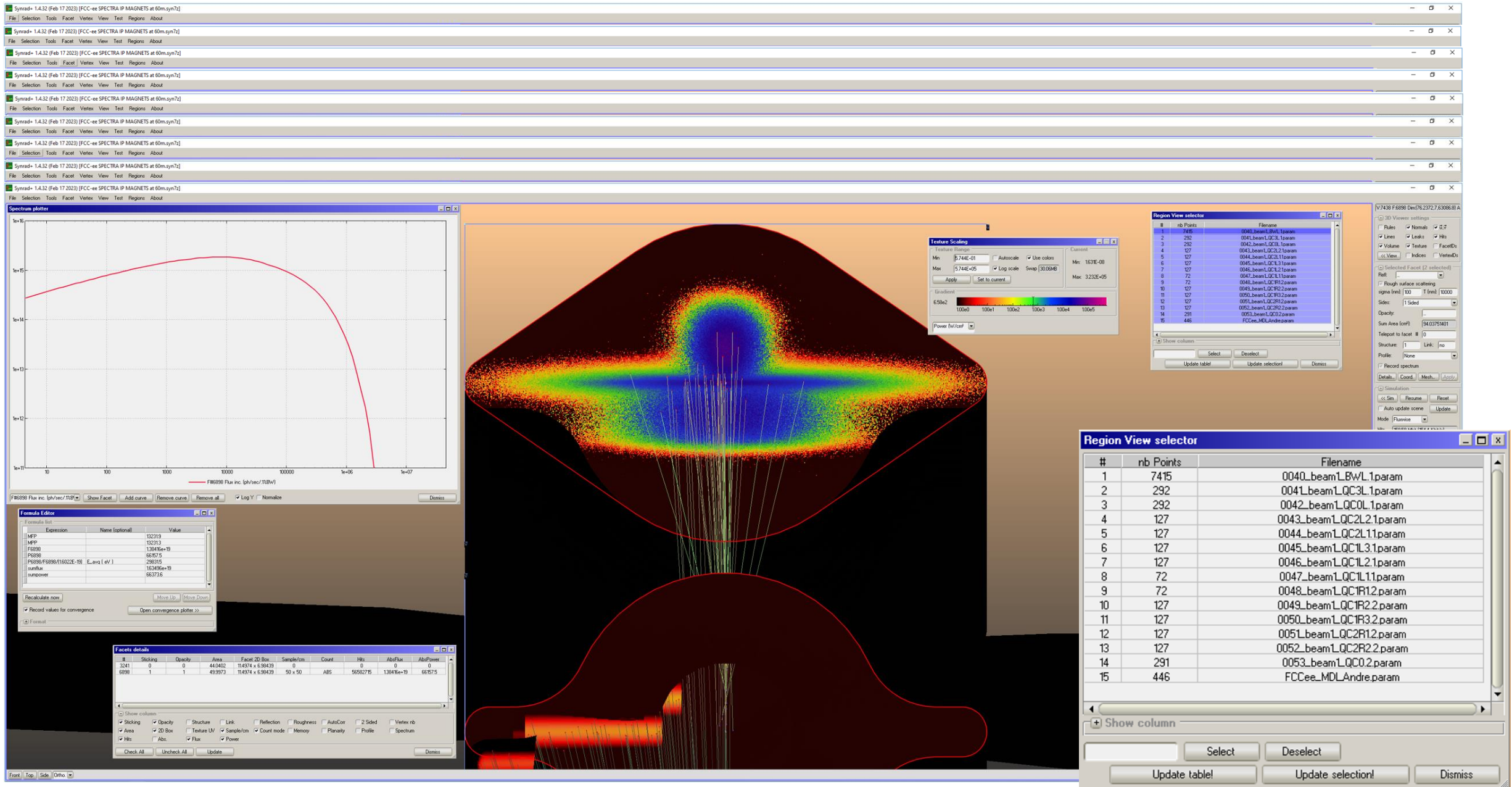


Closing in into the IP region for the no-photon reflection case

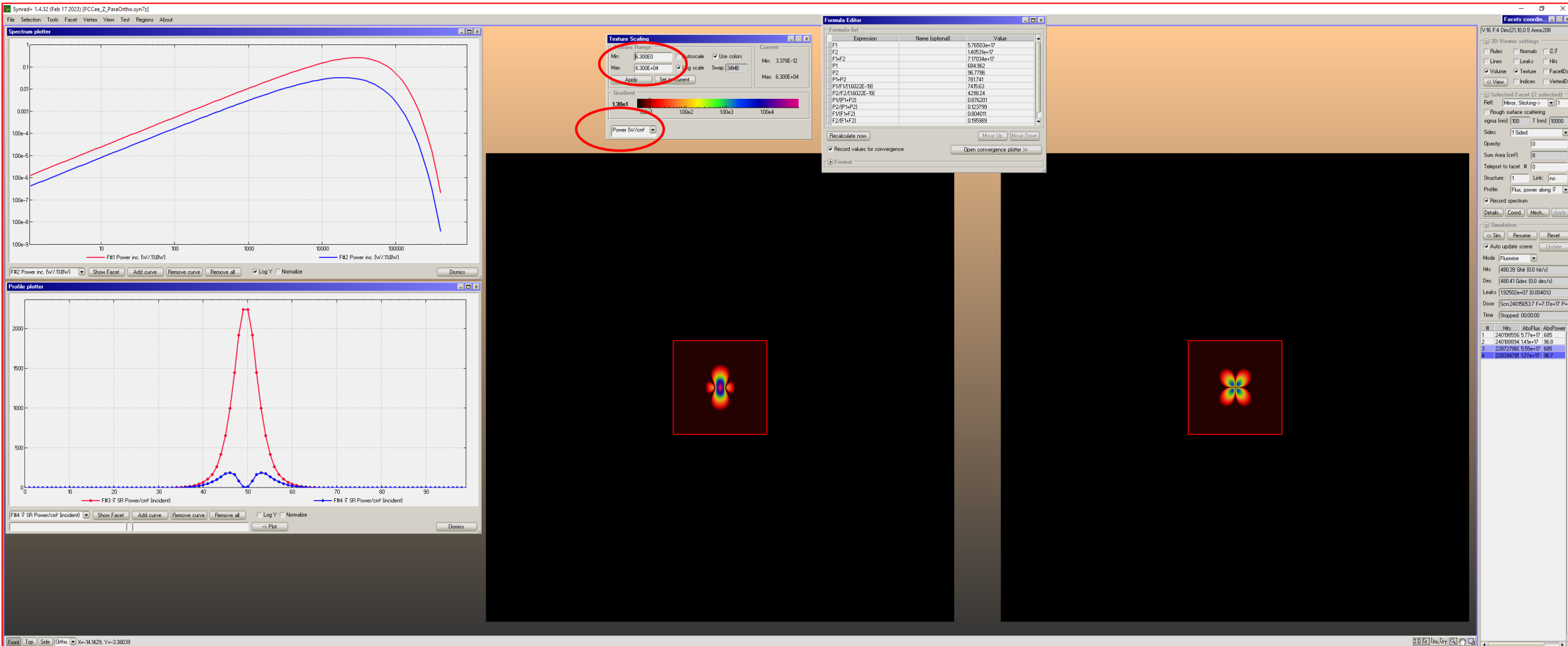


- The horizontally “hourglass” shape of the e- beam is evident →
- The SR along a quadrupole is ZERO when the ideal beam perfectly on-axis and no size, but it grows quickly as the offset from the axis and the bunch size get bigger; **these quadrupoles have very large gradients → large SR emission!**

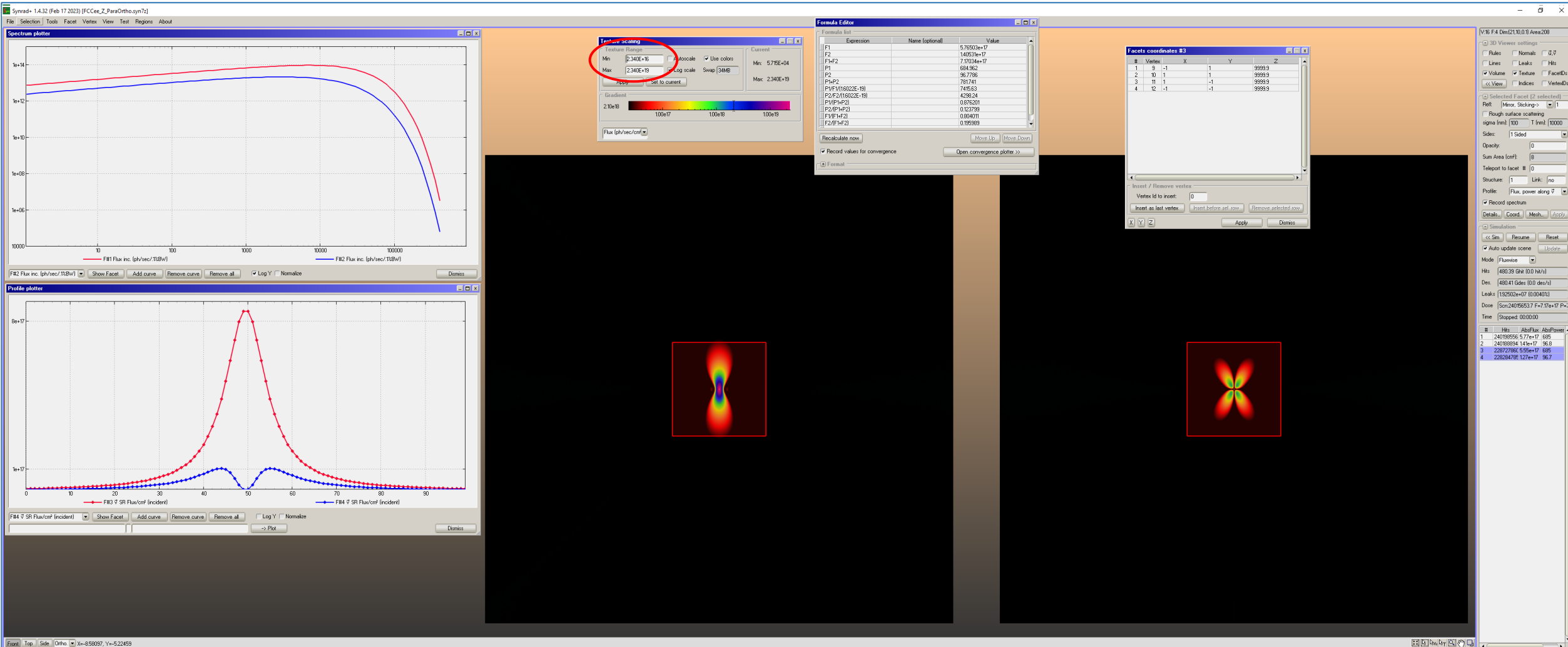
FCC-ee Z: SR Power from different IP magnet sources, reaching a screen at 60 m (facet 6898):



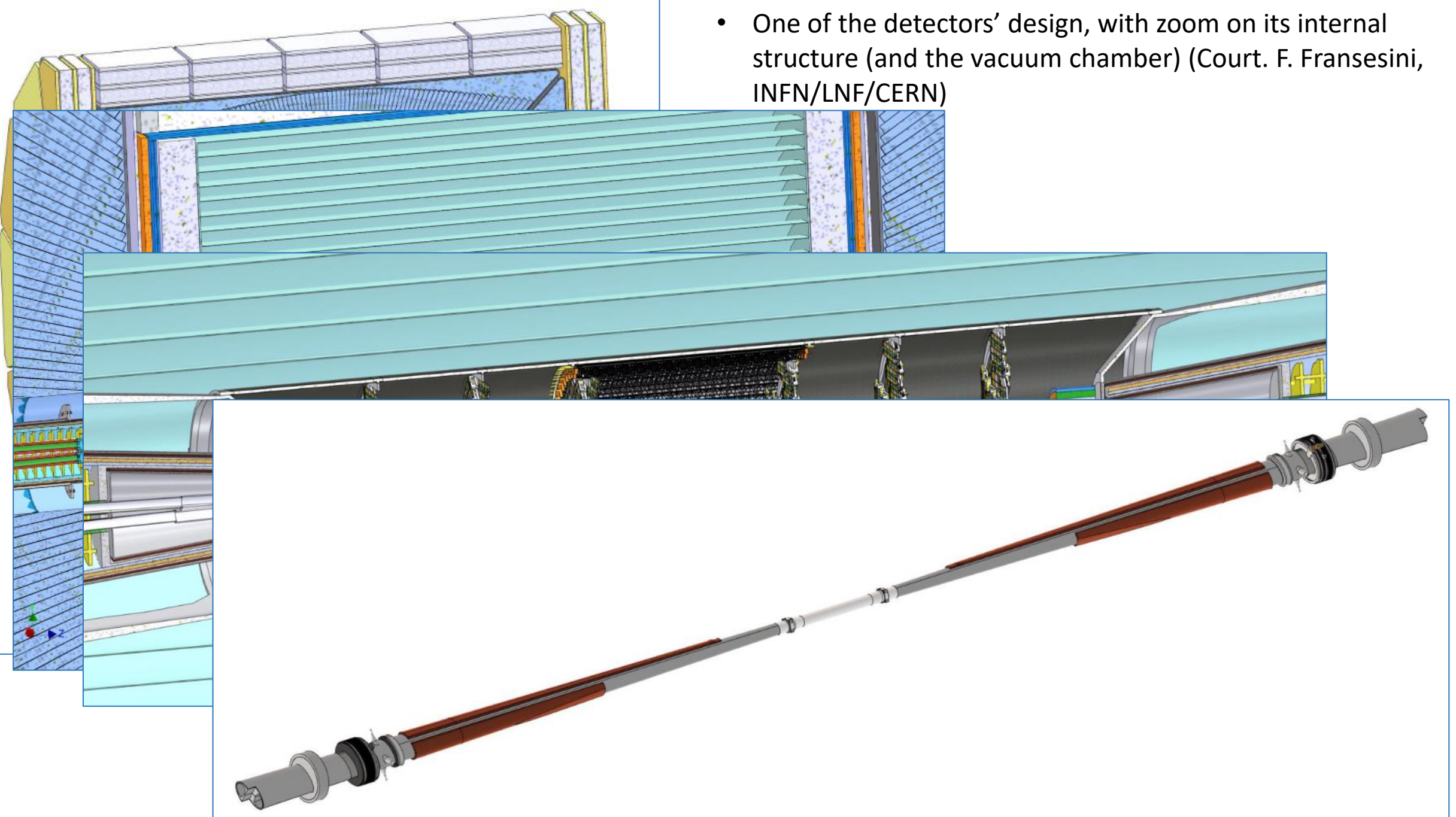
- FCC-ee Z: SR photon **power** distribution at **100 m** from Z dipole, projected on **10x10 cm² (2x2 cm² at center)**, for **parallel (left)** and **orthogonal (right)** photon polarization; IDEAL BEAM CASE, zero beam size, only natural divergence of the SR fan
- Graphs on the left show the SR spectra (in ph/s/0.1% BW/m) at nominal 1270 mA current (above, **RED** is parallel pol., **BLUE** is orthog. polarization), and vertical **power** distribution (+/- 1 cm, smaller square)
- 1 cm corresponds to 0.1 mrad ($1/\gamma=11.206 \mu\text{rad}$); $0.1 \text{ mrad} = 8.92 \cdot 1/\gamma$

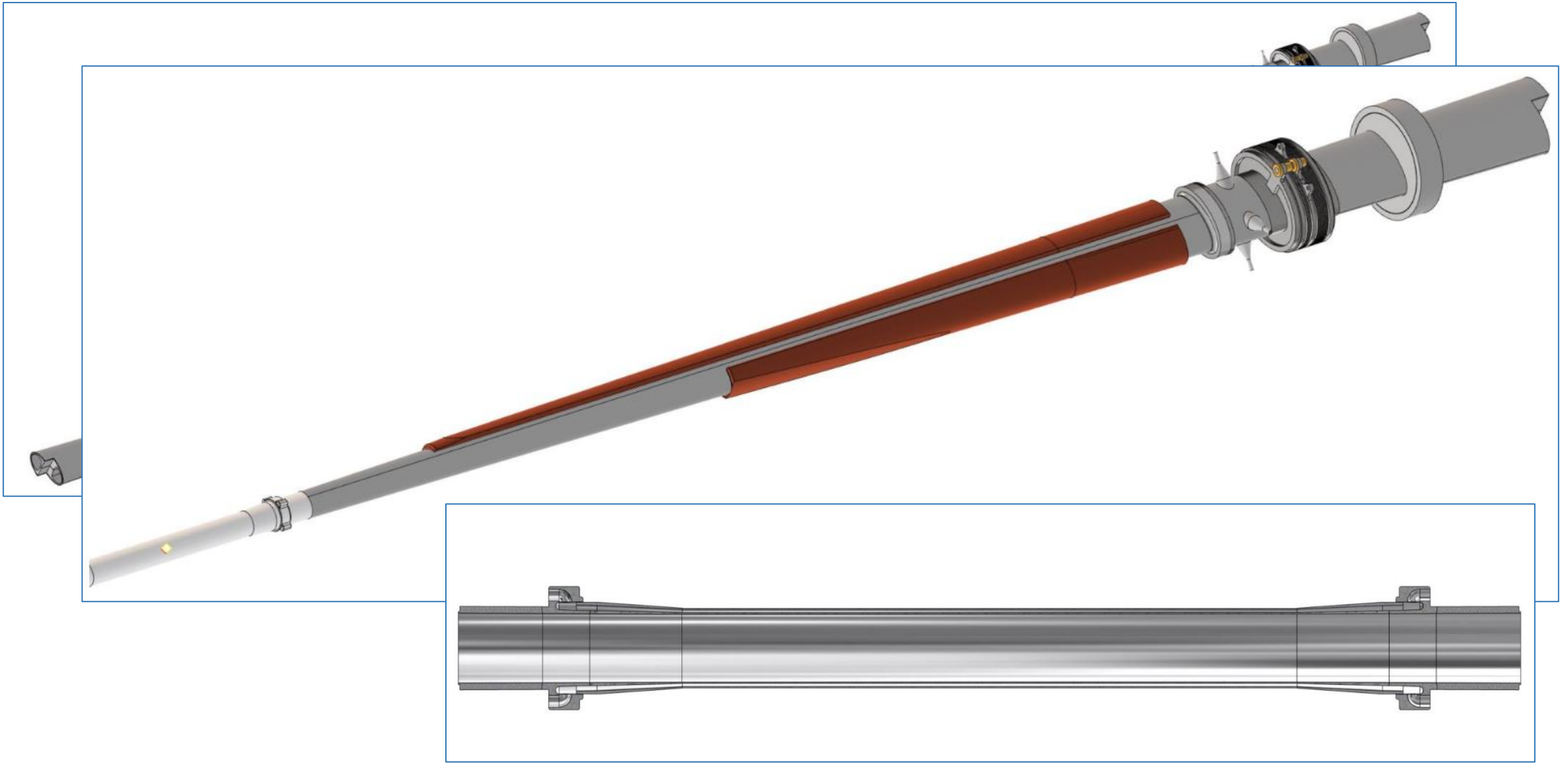


- FCC-ee Z: SR photon **flux** distribution at **100 m** from Z dipole, projected on **10x10 cm² (2x2 cm² at center)**, for **parallel (left)** and **orthogonal (right)** photon polarization; IDEAL BEAM CASE, zero beam size, only natural divergence of the SR fan
- Graphs on the left show the SR spectra (in ph/s/0.1% BW/m) at nominal 1270 mA current (above, **RED** is parallel pol., **BLUE** is orthog. polarization), and vertical **flux** distribution (+/- 1 cm, smaller square)
- 1 cm corresponds to 0.1 mrad ($1/\gamma=11.206 \mu\text{rad}$); $0.1 \text{ mrad} = 8.92 \cdot 1/\gamma$

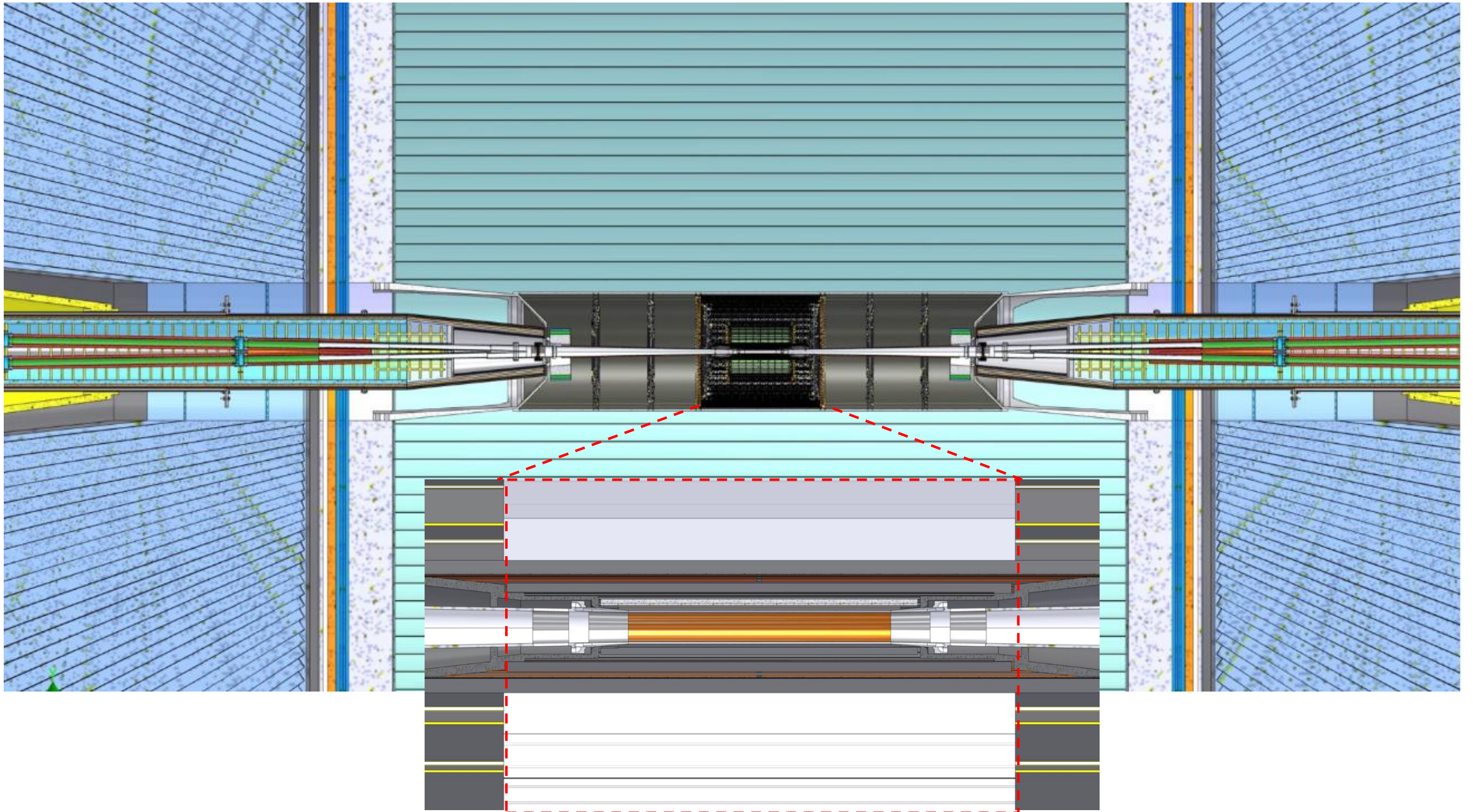


- One of the detectors' design, with zoom on its internal structure (and the vacuum chamber) (Court. F. Franesini, INFN/LNF/CERN)

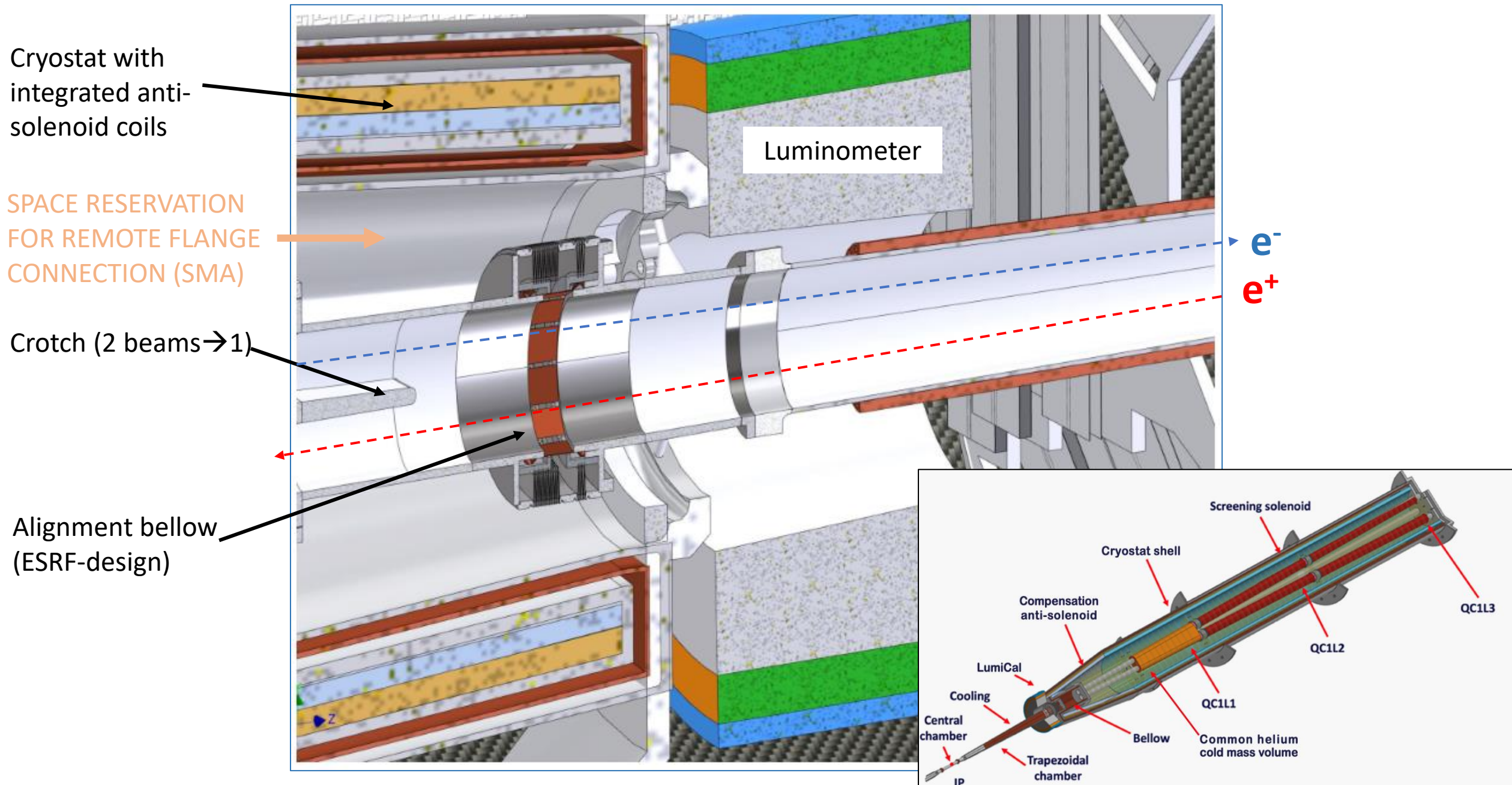




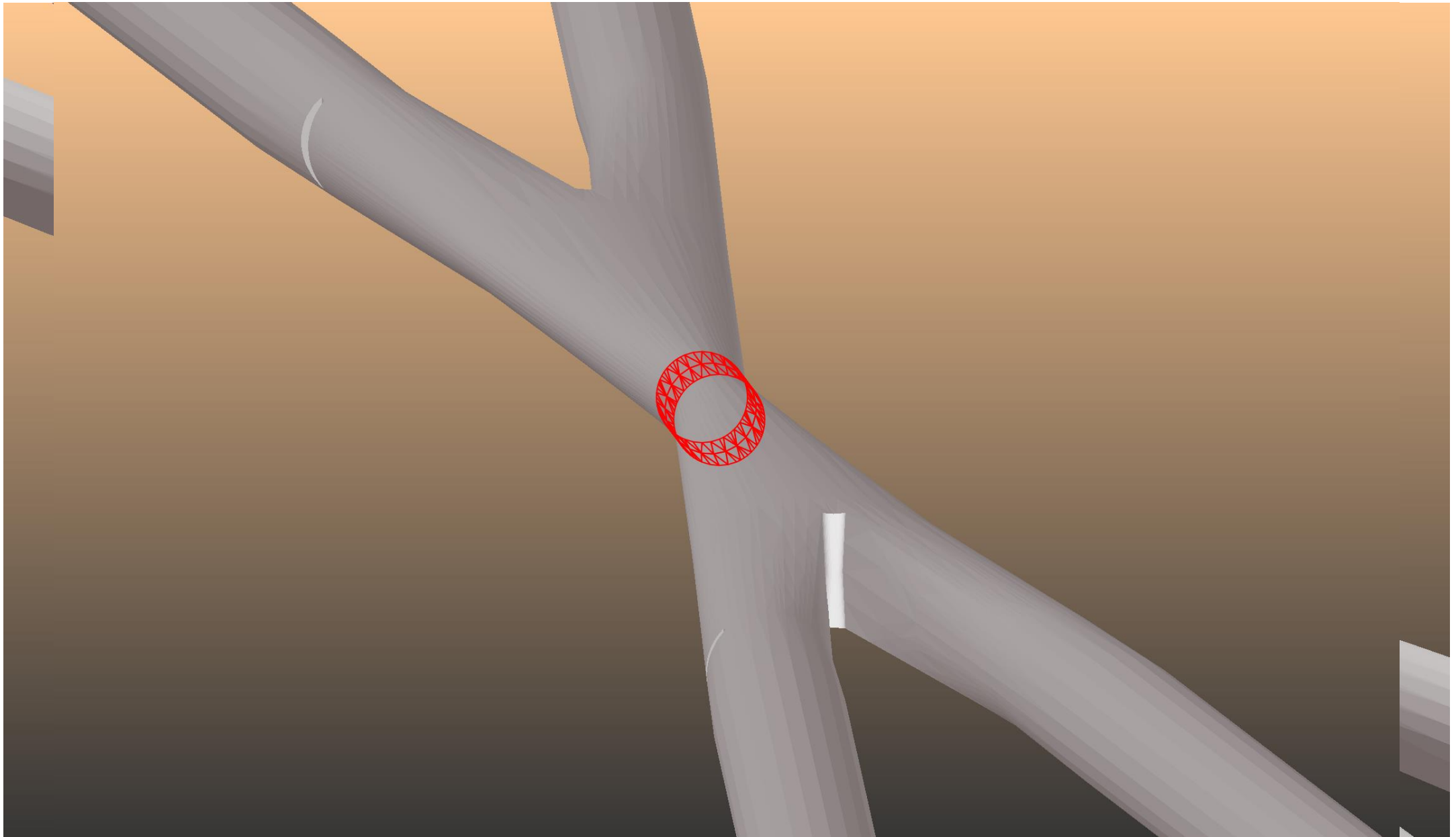
Materials: Albemet (Al-Be alloy); Cu, SS, SS/Al transitions (explosion-bonding), water-cooled;
Central **Be** chamber is **2x9 cm long** only, **double-walled, cooled by paraffin; gold-coated** internally; its internal diameter is **20 mm**



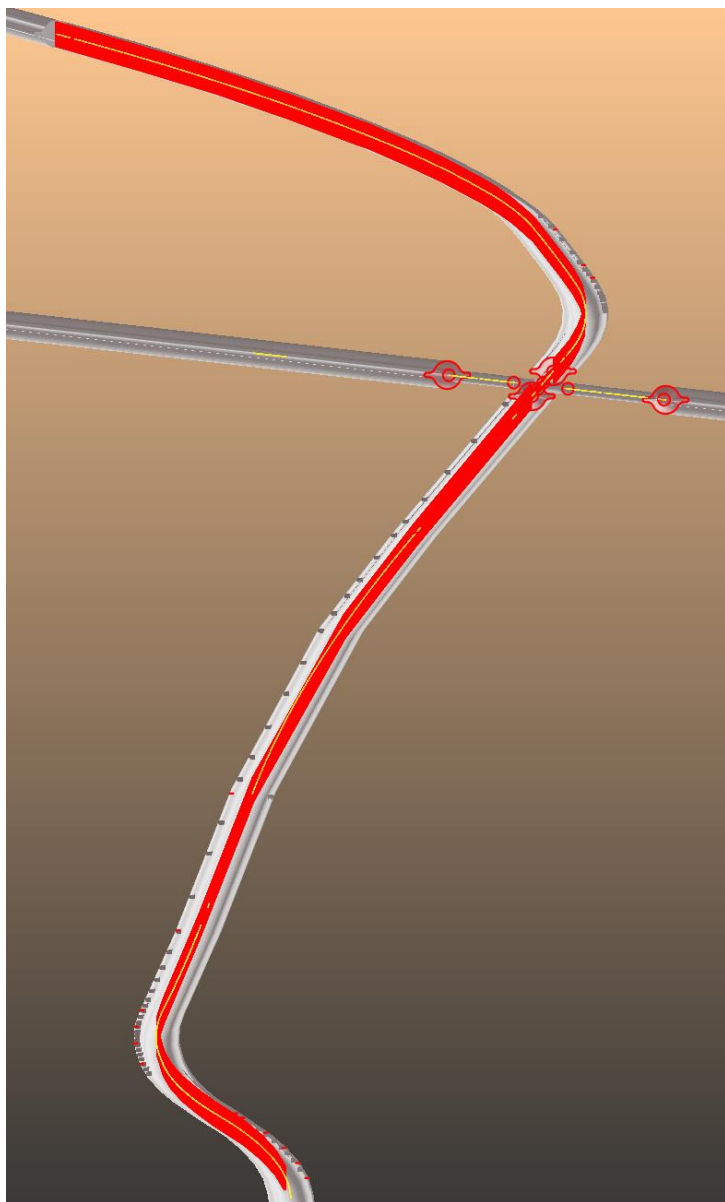
Extremely tight fabrication and alignment tolerances: accurate ray-tracing is a must



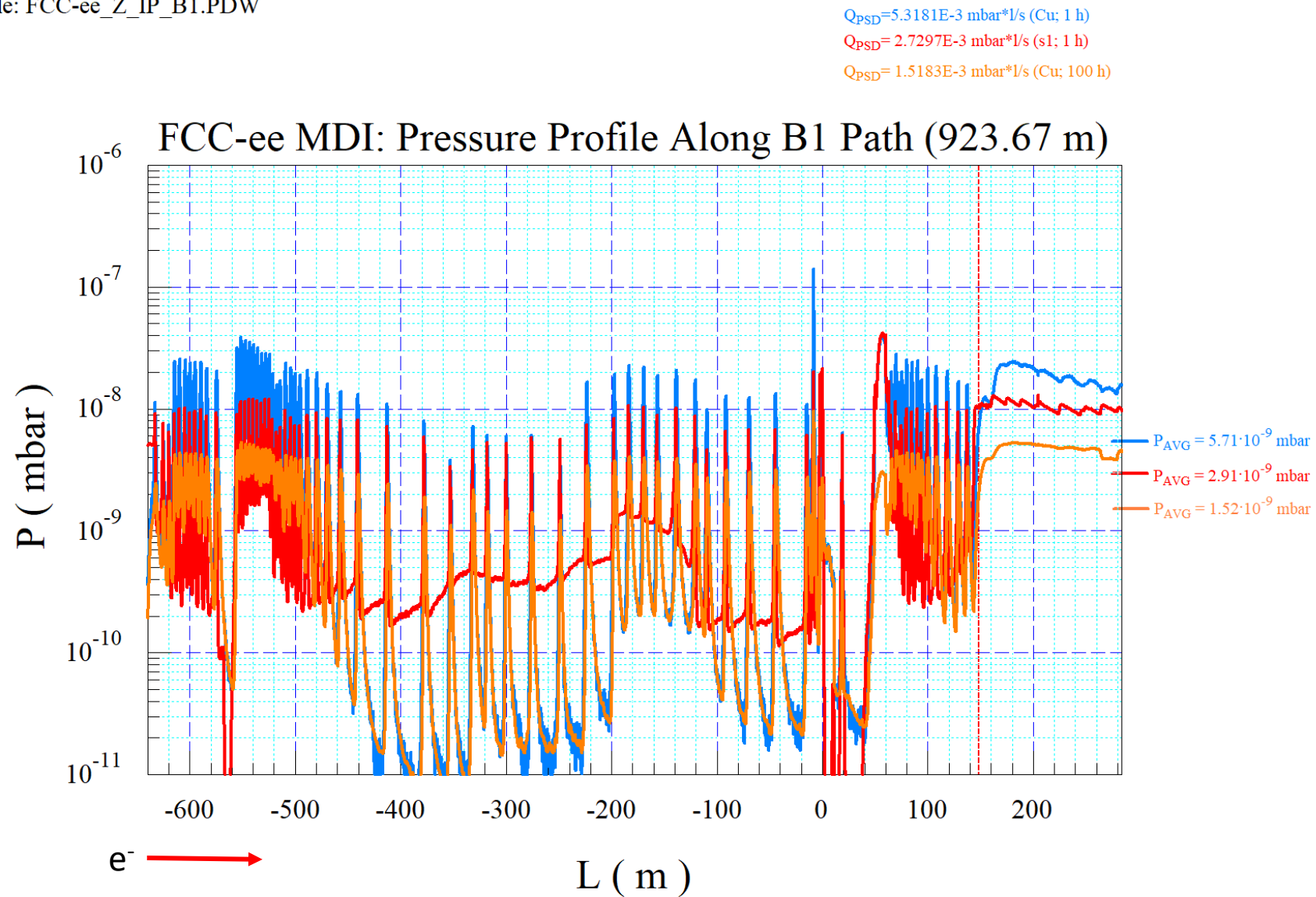
Geometry of the central “X” chamber, as imported from CAD into SYNRAD+ (cour. F. Franesini, INFN/LNF/CERN)



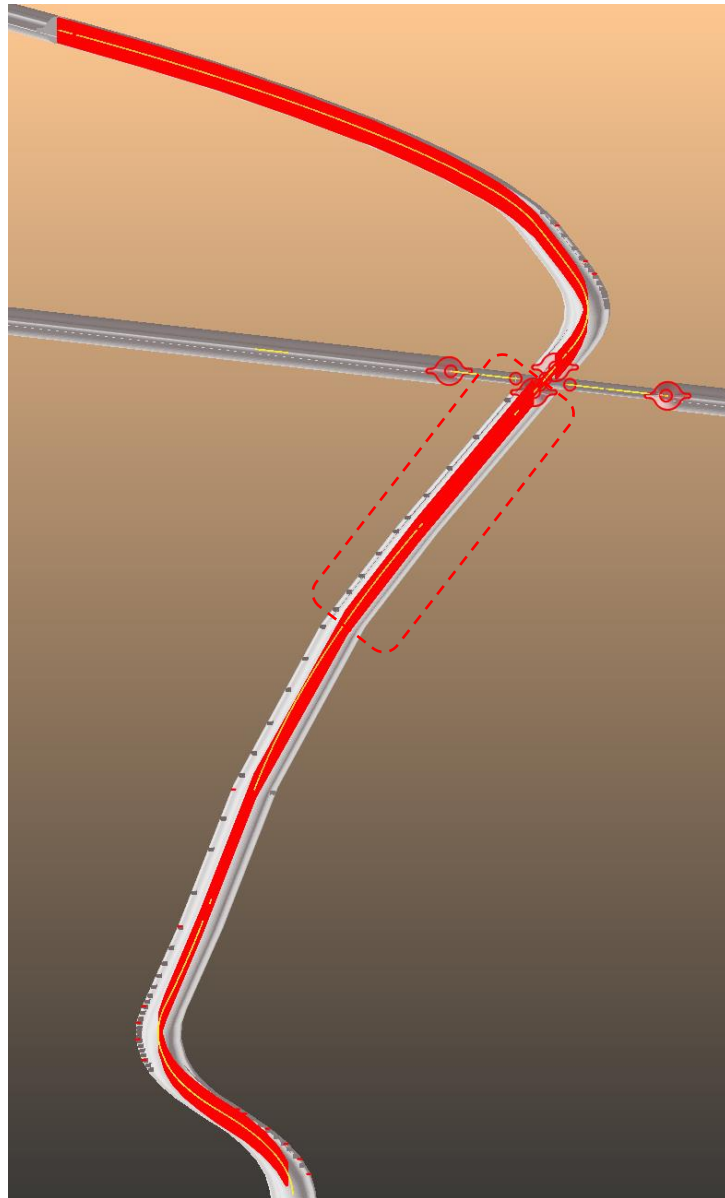
Molflow+ simulation of pressure profiles after 1h (ideal case and Cu reflection) and 100 h (Cu refl.) Cu-like desorption yield with $s=0.008$ NEG sticking coeff.



File: FCC-ee_Z_IP_B1.PDW



Same as previous one but for the 200 m upstream of the IP
Cu-like desorption yield with $s=0.008$ NEG sticking coeff.



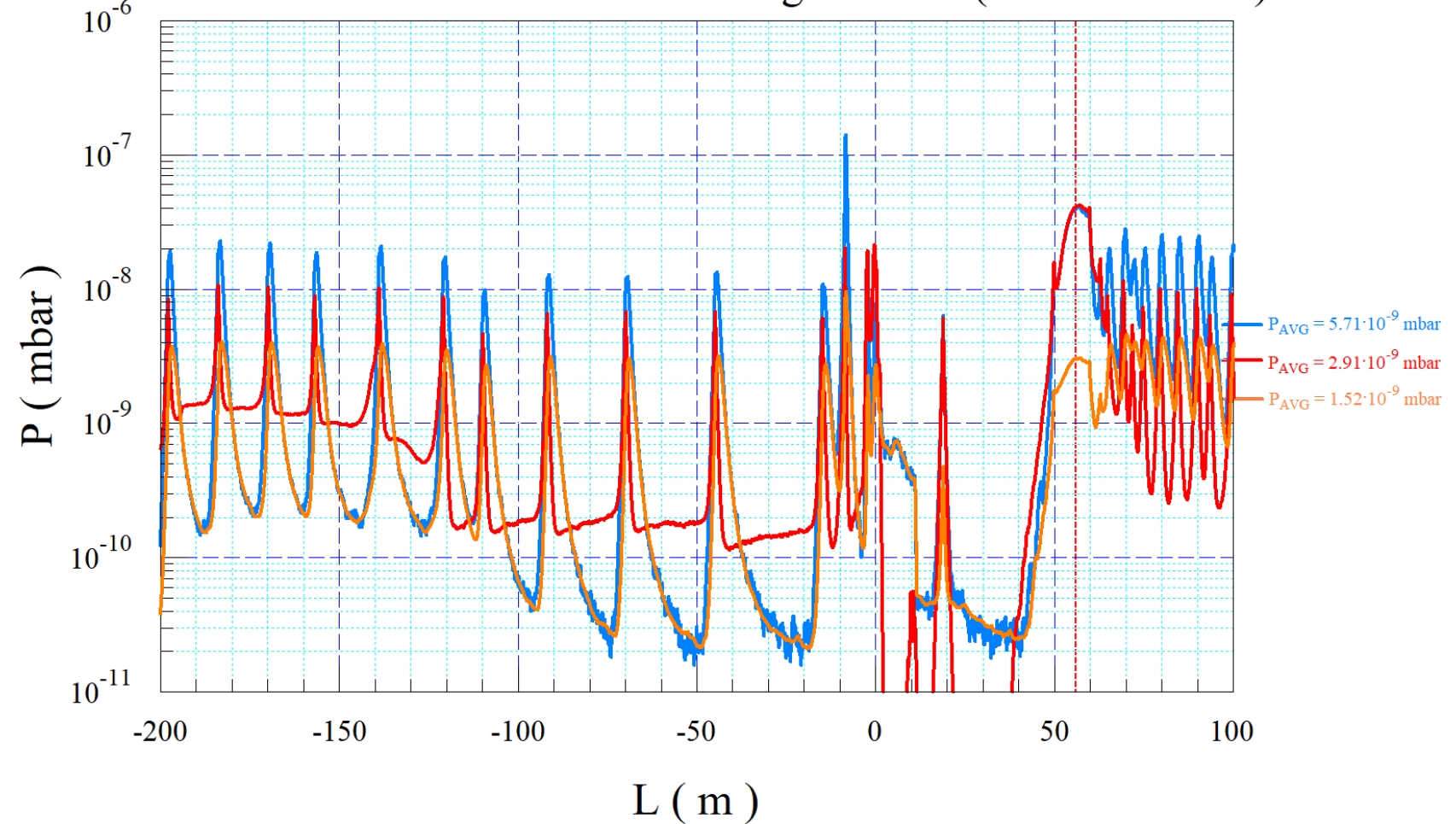
File: FCC-ee_Z_IP_B1.PDW

$Q_{PSD} = 5.3181E-3$ mbar \cdot l/s (Cu; 1 h)

$Q_{PSD} = 2.7297E-3$ mbar \cdot l/s (s1; 1 h)

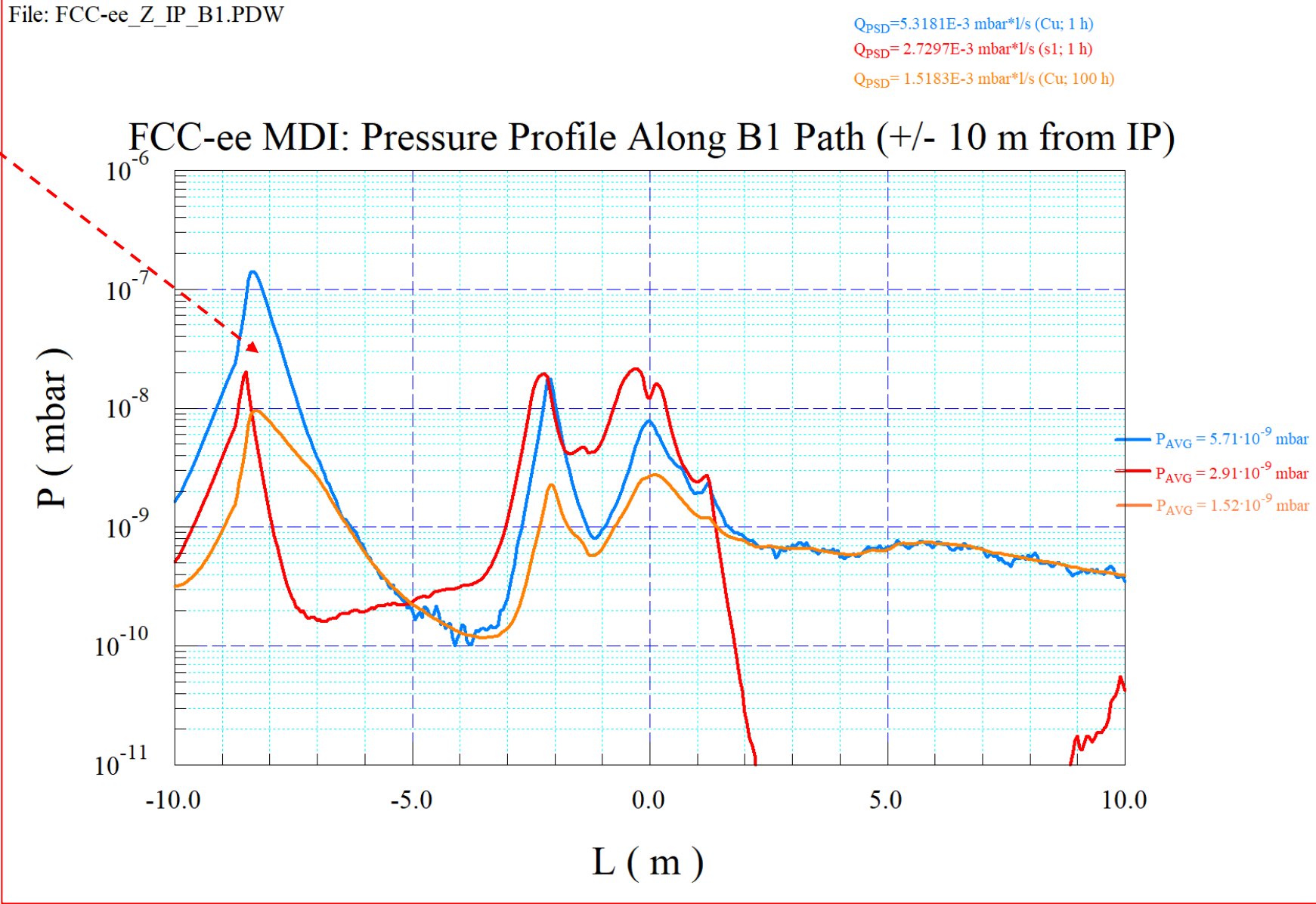
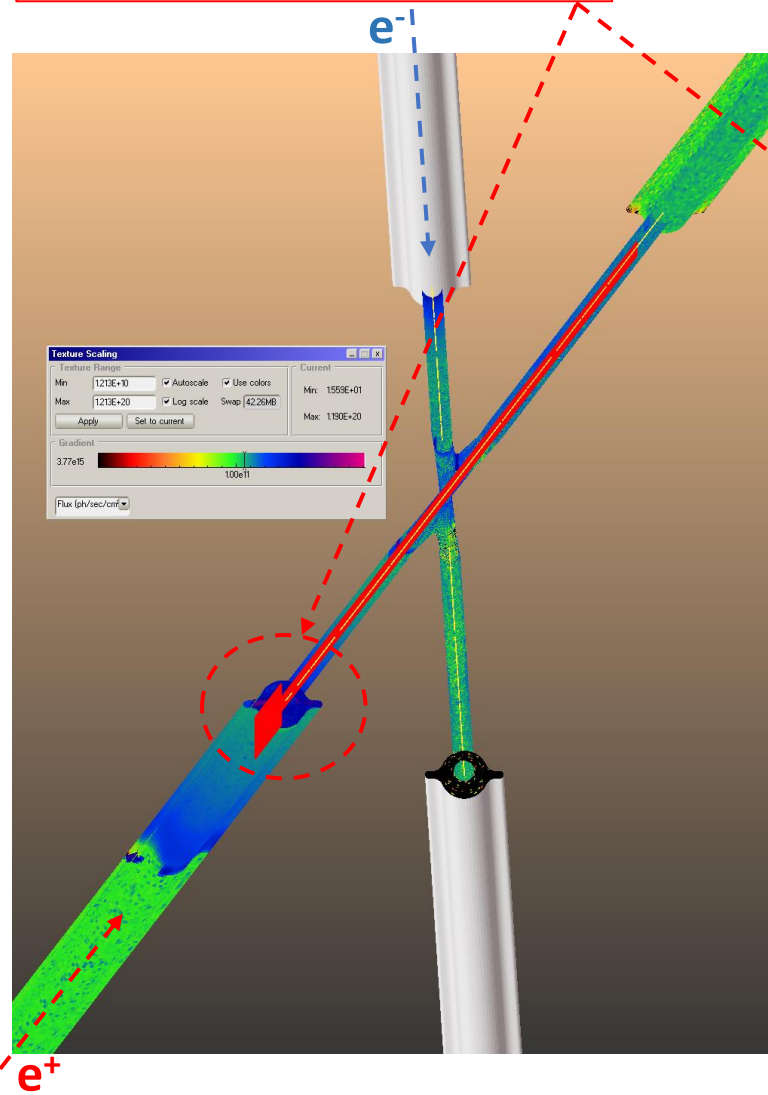
$Q_{PSD} = 1.5183E-3$ mbar \cdot l/s (Cu; 100 h)

FCC-ee MDI: Pressure Profile Along B1 Path (200 m from IP)



This area needs optimization of pumping and trapping of SR-induced desorption by rectangular absorber: e.g. **sawtooth design?**

Same as previous one but for the +/- 10 m to/from IP
Cu-like desorption yield with $s=0.008$ NEG sticking coeff.



Conclusions and future work

- The design of the vacuum system for the MDI region of the FCC-ee collider has progressed quite a lot in the recent years
- We have adopted the same concept as developed for the arc regions, i.e. lumped absorbers catching ~100% of the primary SR photon fans, NEG-coating of all chambers, SMA flanges and BPM buttons, Friction Stir Welding technology, etc...
- The integration of the vacuum system near/inside the detector is proving to be rather challenging due to space constraints, tight alignment tolerances, and need to develop new technologies, e.g. **remote flange connection**
- **Design of the beam- and photon-dump area needs to be looked at**
- Very time consuming ray-tracing calculations, both for the SR fans and the molecular flow, need to be carried out at each change of the magnetic lattice (which happens quite often): an “automatization” of the generation of the vacuum chamber along the MDI will need to be developed (OpticsBuilder, SYNRAD+, Molflow+) → **MANPOWER???**
- The collaboration with different groups is progressing well: integration, lattice dynamics, FLUKA, MDI, magnets, etc...
- **The analysis shown here refers mainly to the MDI at the Z-pole energy: needs to be re-done for the ttbar at 182.5 GeV**
- We are on a good point towards finalizing the design of the MDI vacuum system considering that there are 2 more years prior to the end of this study phase

ACKNOWLEDGMENTS

- The material shown during this presentation has been obtained thanks to a team-work during the last 10 years
- I acknowledge the work of Cedric Garion, Fabrice Santangelo, Christian Duclos, Frederic Luiz, Sam Rorison, Marco Morrone, Fabrizio Niccoli, our machine shop, Marton Ady, Peter Henriksen, Sergio Calatroni, Patrick Krkotic
- Continuous support from FCC and TE management is also acknowledged, never turned down a request
- The collaboration with the FLUKA team (F. Cerutti, B. Humann, A. Lechner et al.) is also acknowledged
- Many thanks to R. Losito for handling our requests for funding for technical development
- Fani Kuncheva-Valchkova, for integration into the tunnel
- Mauro Migliorati and his team at Univ. Rome, for impedance calculations related to chamber components
- Manuela Boscolo and Francesco Franesini, INFN/LNF/CERN, are acknowledged for coordinating the MDI work and providing information and models for the interaction in vacuum chamber
- Andrea Ciarma, Helmut Burkhardt, for data about radiation issues, beam orbits and related loss mechanisms.

